BEN-GURION UNIVERSITY OF THE NEGEV

THE FACULTY OF HUMANITIES AND SOCIAL SCIENCES

DEPARTMENT OF GEOGRAPHY AND ENVIRONMENTAL DEVELOPMENT

The Effect of Rainfall Patterns on Ephemeral Gully Evolution: Using a Landform Evolution Model to Study Short-term Agricultural Catchment Dynamics

THESIS SUBMITTED IN PARTIAL FULFILLMENT OF THE REQUIREMENTS FOR THE MASTER OF ARTS DEGREE

DAVID HOOBER

UNDER THE SUPERVISION OF Prof. Tal Svoray and Dr. Sagy Cohen

September 2015

BEN-GURION UNIVERSITY OF THE NEGEV

THE FACULTY OF HUMANITIES AND SOCIAL SCIENCES

DEPARTMENT OF GEOGRAPHY AND ENVIRONMENTAL DEVELOPMENT

THE EFFECT OF RAINFALL PATTERNS ON EPHEMERAL GULLY EVOLUTION: USING A LANDFORM EVOLUTION MODEL TO STUDY SHORT-TERM AGRICULTURAL CATCHMENT DYNAMICS

THESIS SUBMITTED IN PARTIAL FULFILLMENT OF THE REQUIREMENTS FOR THE MASTER OF ARTS DEGREE (M.A)

DAVID HOOBER

UNDER THE SUPERVISION OF Prof. Tal Svoray and Dr. Sagy Cohen

Signature of student:  Date 27.8.2015

Signature of supervisor: 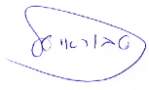 Date 27.8.2015

Signature of supervisor:  Date 27.8.2015

Signature of chairperson

Of the committee for graduate studies: _____ Date_____

September, 2015

Acknowledgments

Writing this thesis has been a fulfilling journey. In Japanese cultural stories, your strength is measured by the amount of friends you have. And to some extent, I am quite strong as many people and friends helped me finish this journey.

First and foremost, I would like to show my deepest gratitude to my advisors. Tal, you said "The art of science is short and on point" – I agreed with that from the start, and that's why we had such great compatibility. You always had an open door while encouraging professional and thought-provoking discussions. Sagy, your insights on each detail combined with open minded approach toward new innovations is what makes you a great advisor. I would like to thank Tom Coulthard for his important input for the CAESAR-Lisflood model and Greg Hancock for reviewing the thesis proposal and his important suggestions. During my GILAB period, I had the privilege to make friends with past and present students. I would like to thank Hodaya Bithan, Galia Barshad and Ofir Miller for the fruitful discussions. A major gratitude is sent to Shai Sela and Michael Dorman for the critical and constructive support. Large gratitude is delivered to Tal Rappaport for the teaching-assistant mentoring, but mostly for the great jokes and times we spent together. I would also like to thank some special friends: Yuval Lorig and Dror Paz for the consultation in geomorphological matters and field protocols. Nitzan Swet for the entire PSA analysis project. And finally, two dearest friend which helped with everything from statistical number crunching to just drinking beer with, Dor Fridman and Rani Mandelbaum. Thanks are extended to several devoted and sun-burned research assistants: Raya Kogan, Lara Ifat Blayink, Eran Grossman, Gil Elboim, Gil Siton, Dorit Bar-Haim, Dror Zolta and Gal Litman. Thanks are also extended to Oron-Moshe Guy, Roni Bluestein, Rachel Zimmermann and Sigalit Gurevitch. To my family, for all your

support – thank you very much. This research was funded by the Soil Sciences Advisory Board of the Israeli Ministry of Agriculture, Grant no. 857-0718-13. We thank the Ministry of Agriculture & Rural Development for "The Whole Organism" scholarship, and the Survey of Israel agency for the topographic layers. Thanks are extended to R.Zaidenberg, B.Yaakobi and Tzabar Kama Agricultural Association for their help in this research.

Table of contents:

List of Figures:

List of Tables:

Abstract

Water driven soil erosion is a major cause of land degradation worldwide. Ephemeral Gullies (EGs) are considered key contributors to agricultural catchment soil loss. Despite their importance, the parameters and drivers controlling EG dynamics have not been adequately quantified. Here we investigate the effects of rainfall characteristics on EG dynamics, using the physically based landscape evolution model CAESAR-Lisflood (CL). CL simulates landscape alteration, induced by erosion and deposition mechanics, on a cell-based data model. In this study, EG evolution was simulated for two rainfall seasons in a 0.37 km^2 agricultural plot situated in a semiarid catchment in central Israel, under seven different rainfall scenarios. Four of these scenarios differ in their overall rainfall volume relative to observed precipitation (+20%, +10%, -10%, -20%). The remaining three scenarios vary in the temporal distribution of rainfall during each storm, allowing us to isolate the effect of rainfall intensity on EG evolution. The results show that: (1) EG depth, length and sediment flux are strongly correlated to changes in rainfall volume, r= 0.99, r=0.89 and r=0.98 respectively, with depth being most sensitive to rainfall oscillations; (2) micro scale morphological behavior varies between rainfall scenarios, resulting in different meandering and connectivity variability; (3) EG evolution is divided into two main stages: an initial rapid development occurring after the first two weeks of the rainy season, followed by a stable development period; (4) a 12 mm $hour^{-1}$ intensity threshold was observed to initiate and, later, modify EGs; and (5) inner storm rainfall variability can have a considerable effect on EG evolution.

1. Introduction

Agricultural catchments worldwide are particularly sensitive to soil erosion that can lead to severe degradation of this valuable resource, with considerable financial and food security repercussions (Pimentel *et al.*, 1995; Garcia-Ruiz *et al.*, 2015). In a review study, Poesen et al. (2003) showed that the contribution of ephemeral gully erosion to soil loss rates can vary between 10% to 94% of all soil loss within catchments, and 50%-80% in semiarid environments (Poesen *et al.*, 2002). Gully erosion is defined as "the erosion process whereby runoff water accumulates and often recurs in narrow channels and, over short periods, removes the soil from this narrow area to considerable depths" (Poesen *et al.*, 2003). Gullies remove soils from hillslopes resulting in substantial contribution to sediment yield (Capra and Scicolone, 2002; Foster, 2005) and limiting proper land-use management by decreasing cropland productivity (Valentin *et al.*, 2005). The damage caused by gully erosion was reported worldwide (De Santisteban *et al.*, 2006; Boardman and Poesen, 2006; Verachtert *et al.*, 2010; Le Roux and Sumner, 2012) but gully development in agricultural catchments has been acknowledged as a major erosion process only in the past three decades (Foster, 1986; Evans, 1993; Zhang *et al.*, 2007).

Gullies are categorized into three groups: (i) permanent/classical, (ii) bank gullies or bank failure and (iii) ephemeral (Poesen *et al.*, 2003; Soil Science Society of America, 2008; Figure 1). According to the Soil Science Society of America (2008), ephemeral gullies (EGs) are defined as "Small channels eroded by concentrated flow that can be easily filled by normal tillage, only to reform again in the same location by additional runoff events".

Figure 1: Ephemeral gully reoccurrence in the Revadim study area.

EG erosion is dictated by an array of environmental factors and processes such as: climate, vegetation, soil properties (Valentin *et al.*, 2005; Huang *et al.*, 2012) and hillslope topography, e.g. contributing drainage area, gully length and gradient (Vandaele *et al.*, 1996; Svoray and Ben-Said, 2010; Svoray *et al.*, 2012). Anthropogenic factors, such as land use change, cultivation method and roads, were also shown to be an important contributor to EG dynamics (Svoray *et al.*, 2015). In order for an EG to occur, an incision at the soil surface must take place, which is typically triggered by land use change (Munoz-Robles *et al.*, 2010), extreme rainfall events (Valentin *et al.*, 2005) or a disturbance caused by agricultural machinery.

Despite of their importance to catchment sediment dynamics and soil erosion (Garcia-Ruiz *et al.*, 2015), space-time gully dynamics (and EGs in particular) are not well quantified in the literature (Poesen *et al.*, 2002; Poesen *et al.*, 2003; Poesen,

2011). This is due to the inherent complexity of these rapidly evolving three-dimensional structures. Advancing quantitative understanding of short-term gully dynamics is an important goal, due to their wide-spread impact on agricultural productivity and sustainability.

A number of models that quantify gullying and calculate the complex erosion processes that contribute to EG evolution and incision have been reported (Merritt *et al.*, 2003; de Vente and Poesen, 2005; de Vente *et al.*, 2013). Merkel et al. (1988) were likely the first to suggest a numerical model that describes soil loss due to EG development. Their Ephemeral Gully Erosion Model (EGEM) uses a combination of empirical relationships and physical equations to compute the EG cross-sectional dimensions (Woodward, 1999). The model requires the exact spatial location of a gully and its length, and can only predict the evolution of its width (Nachtergaele *et al.*, 2001). Alonso et al. (2002) presented an analytical model able to predict scour and migration of headcuts at scales of rills as well as EGs at hillslopes. This model is limited to two-dimensional headcut retreating at a steady rate in homogeneous cohesive soil layers. Gordon et al. (2007) presented a practical model as an improvement to the EGEM drawbacks. The Revised Ephemeral Gully Erosion Model (REGEM), applied within the AnnAGNPS (Annualized Agricultural Non-Point Source) modeling framework, enables soil erosion and runoff simulation within agriculture basins under various scenarios (Gordon *et al.*, 2007). This model is limited as it requires the identification of gully heads in space beforehand (manually or semi-manually) at the catchment sub cells outlet (Gordon *et al.*, 2007).

Landscape Evolution Models (LEMs) can simulate soil processes driven by water based erosion over 1,000 to 1,000,000 years (Willgoose *et al.*, 1991; Tucker and Hancock, 2010; Hancock *et al.*, 2010). A few attempts were made to integrate soil

formation processes at the hillslope scale within a LEM framework. Flores-Cervantes et al. (2006) presented a gully erosion component within the CHILD model, which calculates the headcut retreat of gullies and is implemented within a 3D soil-LEM framework for soil erosion. Another effort is the mARM3D, which consists of coupling soil profile evolution with surface processes (Cohen *et al.*, 2010). The Model for Integrated Landscape Evolution and Soil Development (MILSED) couples both pedogenetic and geomorphic processes (Vanwalleghem *et al.*, 2013). MILSED does not include state-of-the-art sediment and runoff routing mechanics. Further, all three models were mostly applied over relatively long time scales and do not favor prediction of gully formation over relatively short timeframes such as one or two growth seasons. The tRIBS-erosion model developed by Francipane (2012) holds great potential in answering the gaps mentioned. The tRIBS-erosion model is a spatially distributed Triangulated Irregular Networks-based Real-time Integrated Basin Simulator (Ivanov *et al.*, 2004) coupled with elaborated hillslope and channel erosion mechanics. However, even though it represents various robust elements, its predictions over short time scales were found unsatisfactory, and its computational efficiency was found to be low (Francipane *et al.*, 2012). Despite the potential of such three-dimensional soil-landscape evolution models for EG evolution modeling, it is evident that there is a lack of studies which incorporate detailed soil-landscape evolution processes at short temporal scales.

Coulthard et al. (2012) demonstrated the potential of explicitly coupling soil erosion and landform evolution using the Cellular Automaton Evolutionary Slope And River (CAESAR) model (Coulthard *et al.*, 2002; Van De Wiel *et al.*, 2007) by downscaling both temporal and spatial scales. CAESAR has since been modified and undergone several improvements: its latest version, CAESAR-Lisflood (CL), is an

improved physically-based LEM which simulates erosion and deposition processes in river catchments over several time scales using geomorphological process-based calculations. Hancock et al. (2015) showcased comparability between the CL and SIBERIA models. SIBERIA simulates landscape alteration using a set of mathematical equations describing fluvial erosion (Willgoose *et al.*, 1991). While they attained similar results overall, CL was shown to be advantageous by having enhanced sediment transport mechanics, detailed grain size description and elaborate hydro-dynamic representation, while employing hourly rainfall data. A summary of all models reviewed in this thesis can be found in table 1.

In this paper we use CL to investigate the effect of rainfall patterns on EG space-time dynamics in an agricultural plot in the center of Israel. In Section 2, we briefly describe how CL operates and was calibrated for short-term EG evolution modeling and explain our modeling strategy. Section 3 synthesizes the results of the simulations. Last, we discuss the controls of the different rainfall scenarios, the hydrological and geomorphic insights raised from the calibrated parameters and the limitation within the suggested methodology.

Table 1: Chronological overview of the models reviewed in this thesis.

Model	Year	Limitations
EGEM	1988	Only predicts gully width
SIBERIA	1991	Do not account for hourly rainfall data
Headcut migration	2002	Models only headcut retreat
CHILD	2006	No suspended sediment integration
REGEM	2007	Predefined and manual identification of gully heads
CAESAR	2007	Crude flow algorithm (compared to CL)
mARM3D	2010	Lack of field testing
tRIBS-erosion	2012	High computational cost
MILSED	2013	Simplified sediment and runoff routing mechanisms
CAESAR-Lisflood	2013	Crude vegetation component

2. Materials and Methods

2.1. Study Area

The study area is a small (0.37 km^2) agricultural plot (Figure 2) adjacent to Revadim village (Agam *et al.*, 2015), in central Israel (34°49'26.311"E, 31°45'57.171"N). The plot was chosen due to inexistence of road/vehicle pathway intrusion. By doing so, we exclude irregular hydrological behavior on highly contributing runoff surfaces such as tractor roads, thus reducing uncertainty within the CL calibration. The plot acts as a small watershed, confining northwest drainage. Elevations range between 98 to 116 meters above mean sea level. The area is characterized by gentle topographic slopes (0 to 13 degrees) which are translated to a planar landscape with large swales and low hills. These landscape features are the main cause for the reoccurrence of EGs within the catchment at almost the same

spatial location (i.e. same fluvial visual pattern), as documented from a series of aerial photos (2003 to 2012, Figure 1). Typical linear features such as furrows and grooves are common. The EGs depths range between 3 to 55 cm. The field-site is located at the margin between semiarid and Mediterranean climates (Osem *et al.*, 2009), with an average annual precipitation of 490 mm for 2001 to 2013, derived from the Israel Meteorological Service (http://www.ims.gov.il/). Dominant lithology is Alluvium, Marlstone, Chalk and Kurkar while the soil is composed mainly of dark-brown Grumusol (Gvirtzman *et al.*, 1999). Soil texture consists of average: 17% Clay, 58% Silt and 25% Sand. The area is used for cropland production including wheat, cotton, corn, sunflowers and chickpeas.

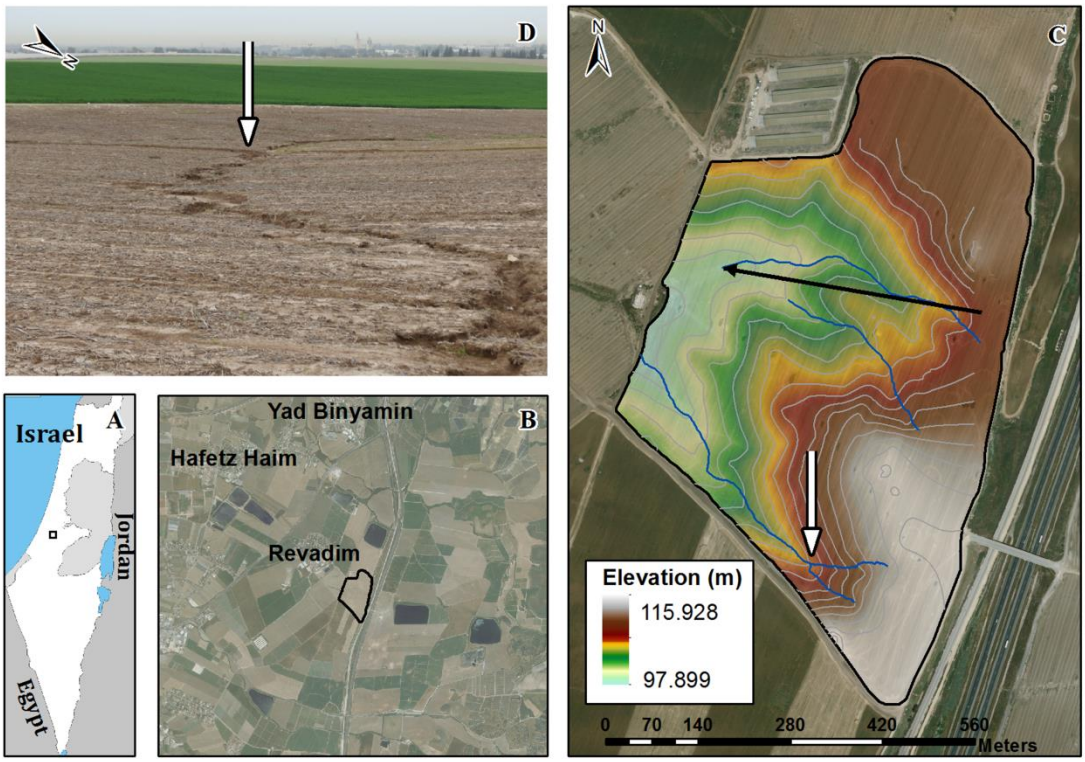

Figure 2: (A) Israel; d-maps.com©; (B) Revadim village; (C) Study site (plot border represented by black line, blue lines represent surveyed gullies, the black arrow represents hillslope flow direction and the white arrow shows referenced branching in the study site; (D) Ephemeral gully branching (indicated by white arrow).

2.2. Modeling

2.2.1. Model Operation

CL simulates geomorphological landscape evolution and landform alteration on a cell-based data model. Each cell is attributed with an elevation value, together forming a numerical terrain representation (i.e. DEM). The alteration process is achieved by routing water across the DEM whilst changing cell elevations according to erosion and deposition mechanics originating from a set of fluvial and diffusive rules (Coulthard *et al.*, 2013b). The alteration is performed as part of a cellular automata concept, in which iteration mechanics are introduced and apply the same set of rules, repeatedly, onto the cellular framework (Figure 3). Consequently, the topography is altered each time step (predefined by the user; usually according to the rainfall input data).

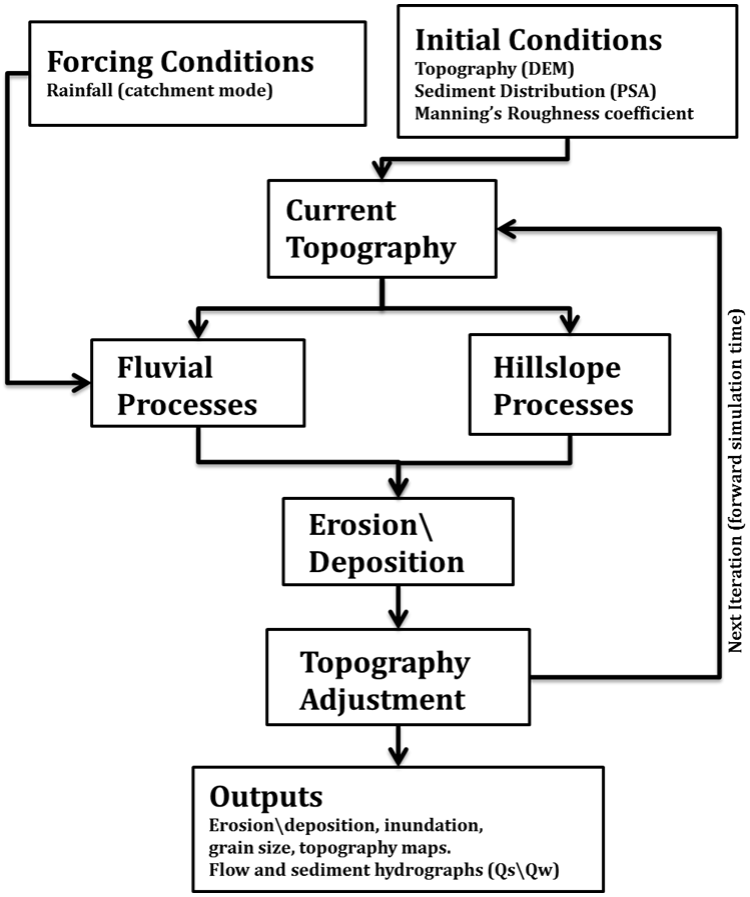

Figure 3: CAESAR conceptual scheme as derived from Van De Wiel et al. (2007).

CL operates in three simulation modes: catchment, reach and tidal. For this study we apply the catchment mode which consists of four main stages. First, the model uses rainfall data to generate runoff using a modified version of the rainfall-runoff TOPMODEL equations (Beven and Kirkby, 1979) for each cell. Runoff calculations take into account the soil moisture store, the rainfall rate and the soil moisture deficit. Second, runoff is distributed as discharge, using the newly added LISFLOOD-FP hydrodynamic flow code, in four directions of each contiguous cell (D4; Manhattan neighbors). Third, flow depth is calculated using Manning's equation and velocity is calculated by dividing water flux between cells by the *hflow* parameter (the minimum water depth at the cell's boundary). Both flow depth and velocity are used to calculate a shear stress threshold that can then be used to calculate fluvial erosion and deposition using sediment transport formulae (Einstein, 1950; Wilcock and Crowe, 2003). Additionally, the model permits a description of as much as nine different grain size classes, which may be transported as suspended or bed-load. Grain size distribution should adequately account for the entire basin's sediment characteristics. Sediment transport is carried out by using an active layer system (Figure 4) comprising of a surface layer representing the gully bed; multiple buried layers representing the stratigraphic unit; and a non-erodible bedrock layer (Van De Wiel *et al.*, 2007). Finally, slope processes are modeled as mass movement occurring when a critical slope threshold is exceeded (immediate slope failure); and soil creep as a function of slope. Sediment from hillslopes is inputted into the fluvial system as well.

The catchment mode requires several input datasets: (i) the starting topography (i.e. initial DEM); (ii) rainfall rate (preferably hourly), spatially uniformed along the basin; (iii) up to nine particle size fraction descriptions and a (iv) bedrock layer

representing the maximum depth at which the soil cannot be eroded further. In this paper we use version 1.6a of CL issued on 19/09/2013.

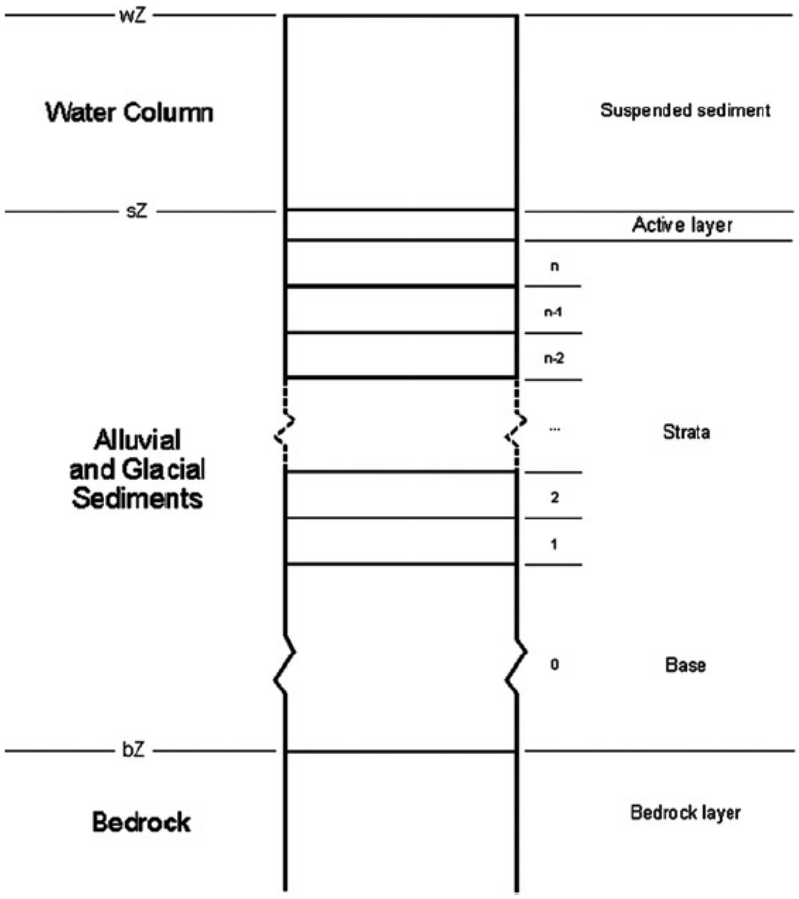

Figure 4: Active layer system as derived from Van De Wiel et al. (2007).

2.2.2. Calibration

Although CAESAR studies typically engage at decadal and millennial scales (Coulthard *et al.*, 2005; Hancock *et al.*, 2010; Hancock *et al.*, 2011; Ziliani *et al.*, 2013; Coulthard and Van de Wiel, 2013; Coulthard *et al.*, 2013a), Coulthard et al. (2012) showed that CAESAR can be used for short time scales. Here we calibrated CL for a short time scale (yearly rainfall season) and a small spatial scale (catchment area of 0.37 km^2) in an agricultural catchment plot. We simulated EG evolution for two consecutive rainfall seasons (Figure 5). The first year was used for calibrating the model and the second year for validation.

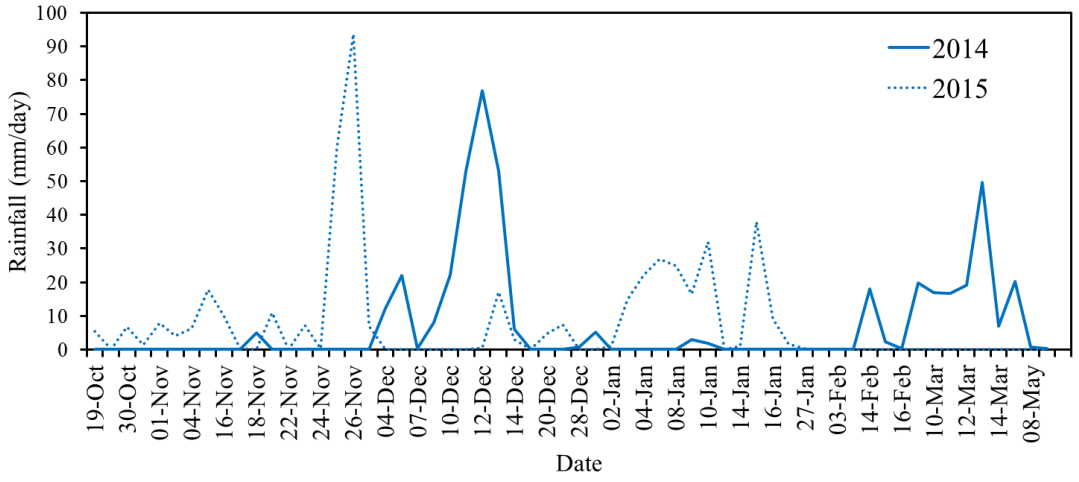

Figure 5: Daily rainfall data for the simulated years.

CL consists of more than thirty individual parameters, rendering a wholesale sensitivity analysis impracticable (Ziliani *et al.*, 2013). Thus we based our calibrations on previously published values with fine-tuning for our field site using a parametric study of key model parameters (Table 2). We favored the values published by Coulthard et al. (2012), for this was the only study found to apply CAESAR within a short time-scale (it was however CAESAR oriented only - i.e. an older version of CL). Recently, Hancock et al. (2015) published a set of values for CL parameters. Although applied for a long term time scale, some of the values are relatively similar to the Coulthard et al. (2012) study. We conducted the parametric study based on these two sources as referenced values. The short-term temporal and spatial scales, and thus the short simulation runtime (~10 minutes), allowed us to conduct hundreds of changeable simulations. In each simulation, we implemented a change of a single value for a specific parameter while other parameters were used as handles (i.e. no cross-parameterization was conducted). Each parameter was given a range of values that were defined according to the base values mentioned above and interpolated according to our understanding.

Table 2: The model parameter values best suited for our small-scale study site. The values are compared to two other published studies using the old CAESAR model (Coulthard *et al.*, 2012) and a large-scale gully erosion study using the new CL model (Hancock *et al.*, 2015).

Parameter	This study	(Coulthard *et al.*, 2012)	(Hancock *et al.*, 2015)
Active Layer Thickness (m)	0.1	0.05	0.02
Courant number	0.2	-	0.7
DEM Grid Size (m)	2X2	0.2X0.2	10X10
Input/output difference	1	-	2.5
Lateral erosion Rate	0.0005	-	0.000002
m value	0.02	0.01	0.01
Manning's n Roughness Coefficient	0.04	-	0.04
Maximum Erode Limit (m)	0.01	0.001	0.005
Minimum Discharge (m^3;Q)	0.02	0.00002	-
Rainfall Time Step	1 hour	10 minutes	1 hour
Sediment Formula	Wilcock & Crowe	Einstein	Einstein
Simulation Mode	Catchment	Catchment	Catchment
Water Depth Threshold (m)	0.005	0.002	-

To evaluate parameterization, we compared simulations of various calibration tests. This was carried out by comparing the final elevation difference (ED; the difference in cell elevation at the end of the simulation relative to its original elevation) output map of each calibration simulation. Consequently, the simulation final ED maps were compared visually and numerically. We used the following qualitative parameters to identify the optimally calibrated simulation: (i) the visual

pattern of fluvial active cells should spatially overlap with observed gullies; (ii) connectivity of EGs, represented by adjacent eroded or deposited cells, should be preserved along the EG network drainage; (iii) thin EGs are more favorable (i.e. less cells comprising the width) and (iv) average depths value should be similar to the average depths value received from the field survey. Table 2 presents the critical parameters which were found to be most influential on the CL outputs as suited for a short time scale. The mechanics of these parameters are explained in Coulthard et al. (2006; 2013b).

2.3. Model input and evaluation datasets

The database used in this paper consists of four main input datasets: (i) a 2X2 m DEM, interpolated from 655 Total station survey points; (ii) hourly rainfall data (Figure 5) from two consecutive rainfall seasons (December 2013 to June 2014 and November 2014 to January 2015) derived from the Israel Meteorological Service (http://www.ims.gov.il/), for the Hafetz Haim station located 3.5 km from the study-site; (iii) soil particle size distribution acquired from a particle size analysis (PSA) conducted on six random soil samples within the plot up to 30 cm deep; and (iv) a bedrock depth file.

For input (i), we did not introduce the *burning-in* process to the DEM. The burning-in process, typically applied in LEM applications, involves lowering the elevation of the simulated catchment main channels in the input DEM to enable a predefined water flow. The process was not applied so we can more reliably imitate the topographic conditions at the start of the rainy season (when EGs are not yet present).

For input (iii), a PSA was conducted to produce the soil description (soil texture and structure) needed for CL. The particle size range varied between 0.01 µm to 291.28 µm. Soil composition (Figure 6) consisted of average clay (17.2%); silt (coarse silt, 12.38% and fine silt, 45.42%) and sand (25%), resulting in silt loam texture.Field surveys were conducted in both years simulated in this study (2014 and 2015). The location of each EG throughout the basin was recorded at the end of the rain season by GPS. Readings were taken along each gully at intervals of ~2 meters. For each reading, depth and width were measured using a measurement tape.

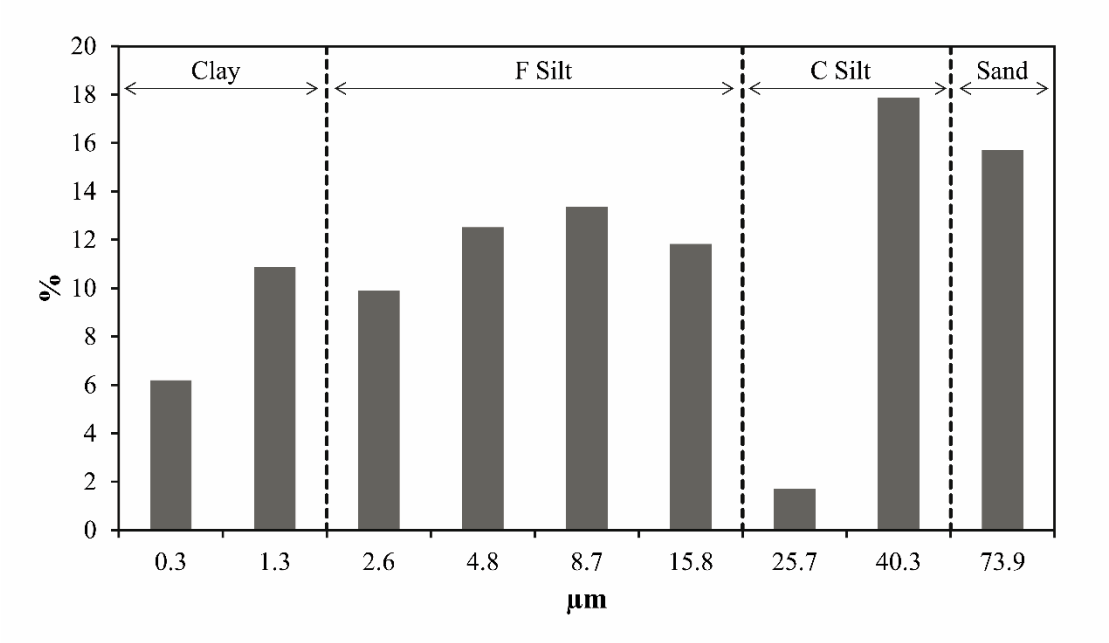

Figure 6: Particle size distribution according to six soil samples, categorized to nine fractions. Dashed lines separate different class weights (clay, fine silt, coarse silt and sand).

2.4. Rainfall Scenarios

The aim of this work was to study the effects of rainfall characteristics including volume, intensity and duration on EG evolution dynamics in space and time. To do so, we employ seven rainfall scenarios (Table 3; Figure 7) whilst scenario 0 (S0) represents observed rainfall data. In scenario 1 (S1) we divide the entire season's rainfall volume (415 mm) by the duration of the entire season (4855 hours), yielding a 0.8444 mm drizzle per hour for the whole season. An additional four scenarios are based on the approach developed by Nearing et al. (2005) of applying a change in rainfall volume in fixed percentage increments. They describe the oscillation of the entire rainfall precipitation volume by fixed increments of +20%, +10%, -10%, -20% (S2, S3, S4, S5, respectively) without affecting duration. In scenario 6 (S6; moderate intensity storms) we divide the rainfall volume of each storm by the duration of the storm (e.g. if a storm of 20 mm occurred along 8 hours, each hour yielded 2.5 mm, reducing the intensity and moderating the peak behavior of each storm). In scenario 7 (S7; high intensity storms) we summed the duration of each storm to a single peak event, as if each storm event occurred within one hour. A summary of the methodology chapter (section 2) is visualized in Figure 8.

Table 3: Rainfall Scenarios. See Figure 7 for visual representation.

Scenario	Description
S0	Observed rainfall data**.**
S1	Season-long rainfall volume averaged by its duration (lowest intensity scenario).
S2	A constant 20% increase in S0 rainfall volume (highest rainfall volume scenario).
S3	A constant 10% increase in S0 rainfall volume (higher rainfall volume scenario).
S4	A constant 10% decrease in S0 rainfall volume (lower rainfall volume scenario).
S5	A constant 20% decrease in S0 rainfall volume (lowest rainfall volume scenario).
S6	Average of each S0 storm volume by its duration (moderate intensity scenario).
S7	Sum of each S0 storm volume concentrated in one hour (extreme intensity scenario).

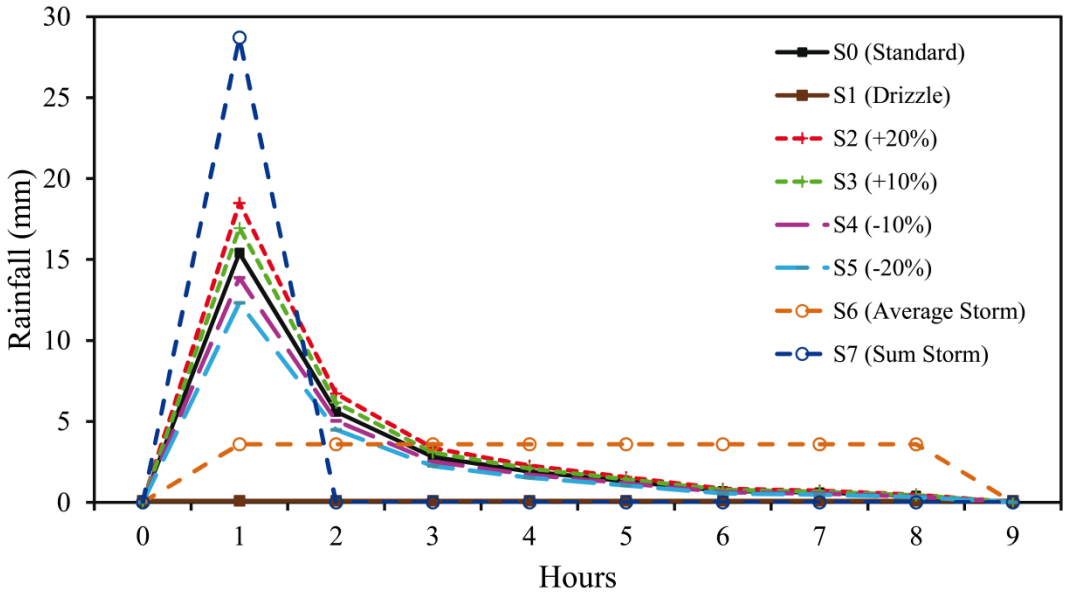

Figure 7: Rainfall time series applied on a singular storm event to visually represent the rainfall scenarios used in this study (Table 3). Observed rainfall values (baseline) are represented by the black line with square symbols; S0. Higher rainfall volume scenarios are marked with a plus symbol. Lower rainfall volume scenarios are marked with a hyphen symbol. Circle symbols represent both scenarios in which observed rainfall changed in duration and intensity, rather than volume. The rainstorm lapsed over 8 hours for a total of 28.7 mm.

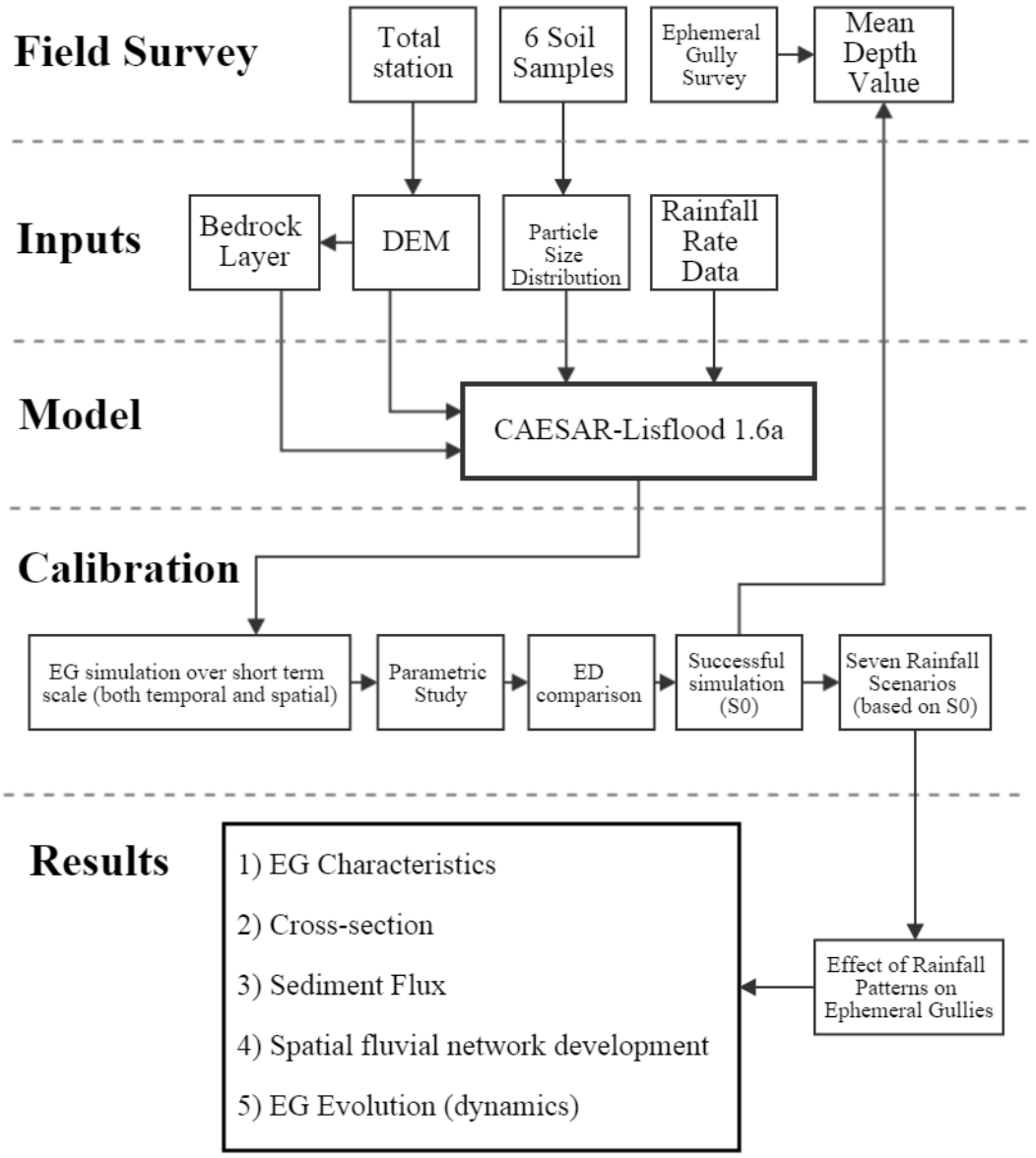

Figure 8: Schematic presentation of research approach and thesis structure.

3. Results

3.1. Model's Predictive performance

We evaluate CL's predictive performance against field-surveyed EGs in our field site. Figure 9a is an output ED map based on utilizing the most favorable calibrated parameterization values (Table 2) discussed in section 2.2.2. Observational analysis shows a good agreement with the model's predictions as: field-surveyed EGs (blue lines) spatially overlap predicted EGs, and the average EGs depths value at the end of

the simulation corresponds well to our field survey of depth value average (14.9 and 12.65 cm, respectively). Further, the prediction preserves the rest of the conditions which were discussed in section 2.2.2: connectivity along the EG network is preserved in most places and eroded areas (red cells) are generally thin. Therefore, spatial fit by observation alone is deemed more than agreeable, as most areas and conditions were successfully predicted and met.

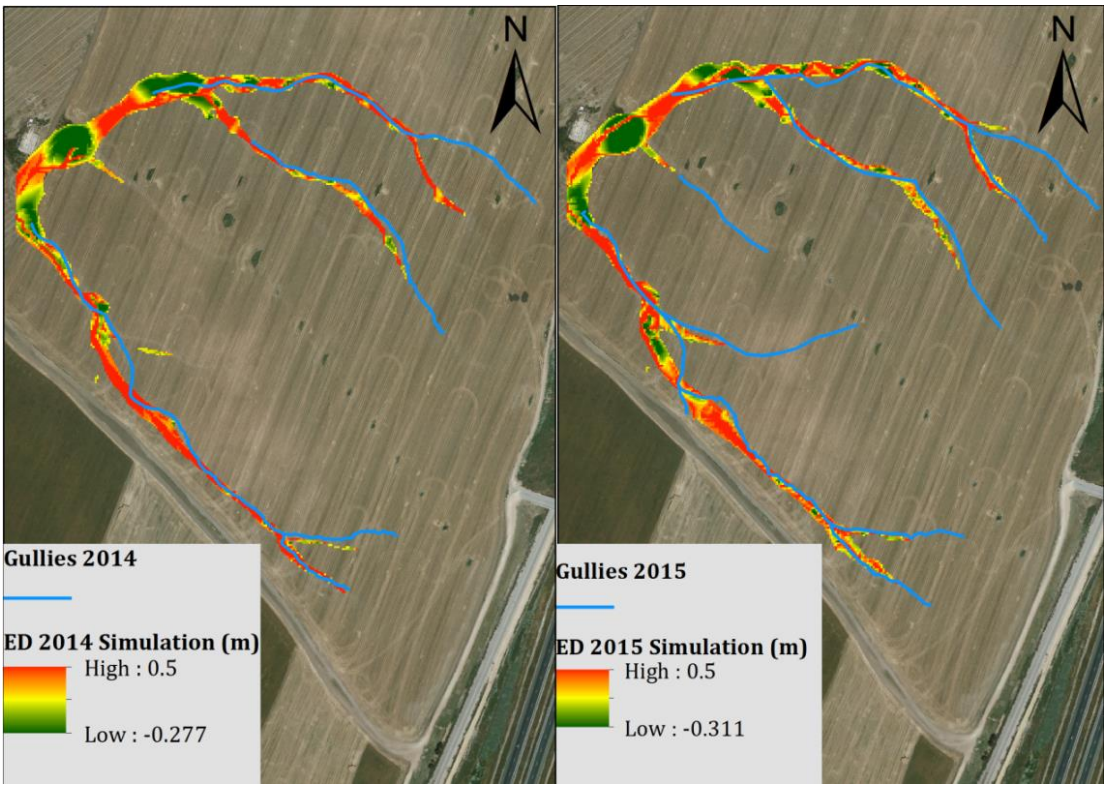

Figure 9: Elevation difference (ED) at the end of the S0 simulation for the (a) 2014 and (b) 2015 rainfall seasons. The blue lines represent field-surveyed EGs in each year. Positive values (red cells) represent erosion and negative (green cells) are deposition.

Most notable prediction errors are the north-west area of the EG network which was erroneously predicted (commission error) and gully lengths/head locations which were not predicted (omission errors). Spatial fit was also validated in the following (2015) rainfall season (Figure 9b). Spatial fit between predicted and observed EGs seems satisfactory as well. However, while the fluvial pattern is very similar, the

surveyed EGs are longer than those surveyed during the previous year. The yearly rainfall volume in 2014 and 2015 was similar, 419.5 mm and 428.5 mm, respectively.

3.2. Rainfall Scenarios

The effects of rainfall characteristics on EG development are explored here based on comparison between the various rainfall scenarios (Table 3) apparent in the model's final ED output maps. The results show some variability in the simulated EG network between the different scenarios (Figure 10). S1 and S7 are the two extreme rainfall intensity scenarios (low and high, respectively; Figure 7). While most scenarios evolved to a fully developed gully network, S1 did not. S7 however shows that large areas were slightly eroded and consequently deposited at the hillslope -this may be attributed to rill erosion.

The remaining six scenarios (S0 and S2 to S6) demonstrate essentially the same fluvial behavior at the macro scale: all scenarios evolved into three main EGs, resulting in similar areas of deposition and erosion and with similar fluvial-evolutional orientation. At a micro-scale a number of differences can be observed: different meandering orientation (which is especially notable in the middle EG), thinner or wider deposition areas, the number of EG heads, connectivity or (dis)connectivity expressed as banding of erosion and deposition (especially in the northern EG e.g. S4 and S5) and depth values variation (e.g. lighter hue scenarios like S6). These results show that higher rainfall intensities tend to preserve high connectivity within the EG network. S6, as a moderate intensity rainfall scenario resulted in lower connectivity. Moreover, S6 resulted in lower EG depths. It is surprising that S4 and S5 (-10% and -20%) are not substantially affected by rainfall volume decrease, expressed by either low connectivity or lower erosion/deposition rates.

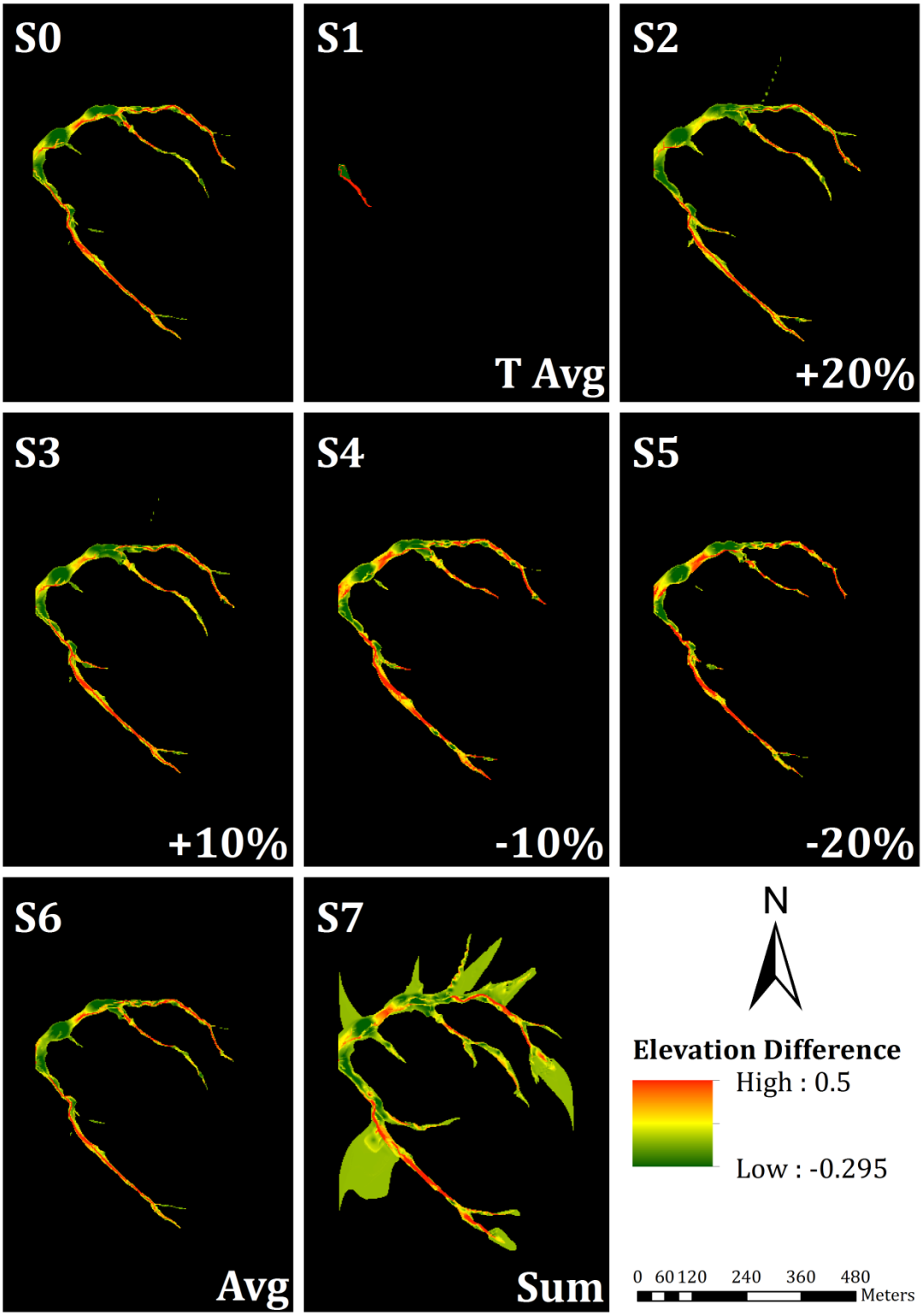

Figure 10: Elevation difference (ED) maps for the eight rainfall scenarios. Positive values (red) represent erosion and negative (green) are deposition.

Three indices are used to quantify the effect of rainfall scenarios on EG development: (i) sum depth - summation of all eroded cell elevation difference values; (ii) sum length - summation of all EG network lengths; and (iii) mean depth - the average of all eroded cell elevation difference values. Figure 11 shows the values of these indices as a departure from the S0 baseline scenario (e.g. a value of 1 is 100% greater than S0). The S1 simulation resulted in -93% and -94% difference for sum length and depth, respectively. S2 and S3 which represent higher rainfall volumes show an increase of 29% and 16% in sum depth respectively, and a surprisingly marginal increase of 13% and 6% in sum length, respectively. The reason for this marginal increase could be that relatively high slopes at the headwaters limit the EGs length.

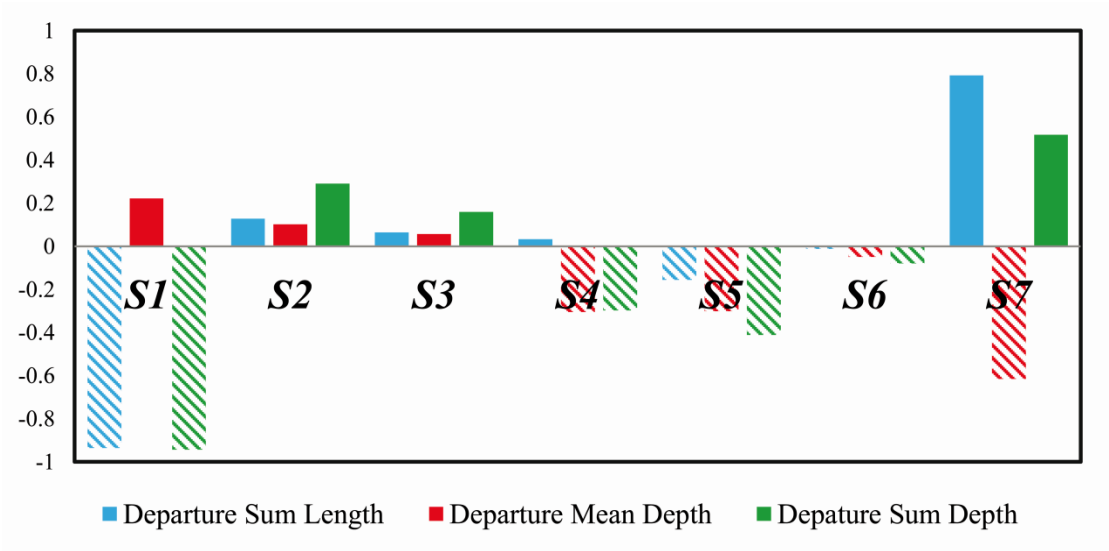

Figure 11: Differences in Sum Length, Sum Depth and Mean Depth between each rainfall scenario and the baseline (S0) simulation. Diagonal fill patterns represent negative values and solid fill, positive values.

S4 and S5 yielded 30% and 41% less depth respectively than S0, which are bigger differences than expected given that the changes in rainfall volumes are -10% and -20%, respectively. This indicates that a decrease in rainfall volume can lead to almost

double a decrease in sum depth (Table 4). Length wise, S4 yields an increase of 3%, which is quite subtle, compared to that expected. The sum length index of S5 was 16% lower than S0. S6 resulted in -1% and -8% changes in length and depth, respectively. S7, the extreme rainfall scenario, yielded massive differences of 79% and 52% in sum length and depth, respectively, due to high intensity over a very short duration. Strong correlations were found to sum length, sum depth and mean depth (r=0.89, r=0.99, r=0.96, respectively; Figure 12) between the rainfall scenarios in which change in volume was the dominant variable (i.e. S2, S3, S4 and S5). The EG parameter most responsive to rainfall volume change is sum depth, indicated by its steepest slope.

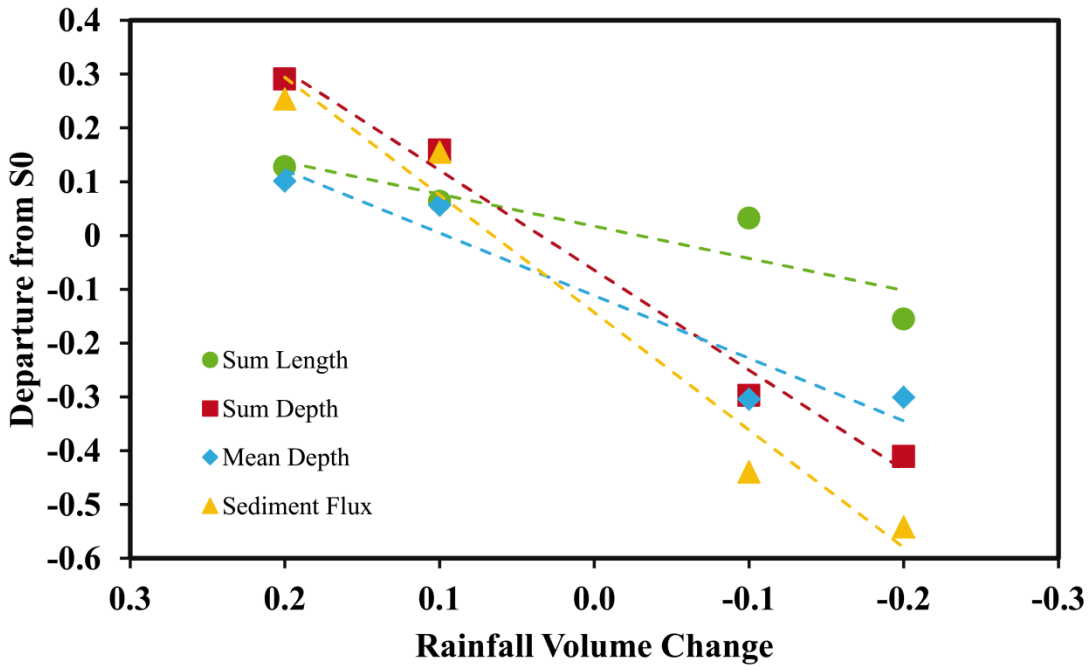

Figure 12: Changes in four EG characteristics (sum length, sum depth, mean depth and mean length) in response to differences in rainfall volume, both relative to the S0 scenario. Coefficient of determination of each character and its corresponding p value are as follows: Sum length (r=0.89; 0.103), Sum depth (r=0.99; 0.006), Mean depth (r=0.96; 0.038), Sediment flux (r=0.98; 0.016).

Mean gully depth was also examined. This index was expected to show similar trends as sum depth and length, and in most scenarios this was indeed the case. However, the most apparent change in mean depth compared to S0, 22%, was found for S1, which represents the lowest intensity scenario (i.e. drizzle scenario). S1 was a far less erosional scenario compared to S0, however, when erosion did occur, it was at relatively high magnitudes. This means that even if the length of the EG was relatively short, the gully itself evolved to a significant mean depth of 19 cm. This is plausible yet not expected, and is probably due to the spatial variance of mean depth that is calculated from all eroded cells. This is also supported by S7 which is the most eroded scenario. However, the slightly eroded hillslope areas in S7, substantially lowers the mean depth. This implies that mean depth is perhaps not an ideal index to imply on EG development; however it is used since it is more readily comparable to the field survey.

Table 4: Summary of the changes in sediment flux (Qs), sum length, mean depth and sum depth, according to each scenario.

	S0	S1	S2	S3	S4	S5	S6	S7
Rainfall volume increase/decrease	0%	-	+20%	+10%	-10%	-20%	-	-
Sediment flux	0%	5.595%	25.35%	15.53%	-43.9%	-54.13%	-8.58%	41.82%
Sum Length	0%	-93%	30%	6%	3%	-16%	-1%	79%
Sum Depth	0%	-94%	29%	13%	-30%	-41%	-8%	52%
Mean Depth	0%	22.2%	10.1%	5.7%	-30.4%	-30.1%	-4.9%	-61.5%

A simple index was compiled to normalize the effect of the rainfall scenarios on EG characteristics, regardless of the modified variable (duration, intensity or volume). The index (termed *D,* Equation 1) consists of four simple rainstorm characteristics: Rain intensity, Hours Lapsed, Rainfall volume and standard deviation:

$$D = b_1 R_I b_2 HL b_3 R_V b_4 R_{sd} \quad (1)$$

For this initial attempt, all components were assigned with equal weights (i.e. b_1=b_2=b_3=b_4=0.25). The D index was applied for one storm (as most rainstorms were found to have similar intensity ratio, r^2 = 0.88; Figure 13). The results show strong positive correlations between D and sum length and depth (r^2=0.96 and 0.93, respectively; Figure 14a and 14b). Correlation to mean depth resulted in a lower correlation, r^2=0.39 (Figure 14c). This demonstrates the strong influence of rainfall characteristics on EG evolution and that a simple predictive empirical model can be developed to quantify these relationships. More research is needed to estimate the universal applicability of such approach as it is expected, for example, that basin characteristics will have a major effect on the relationship between the rainfall and EG characteristics.

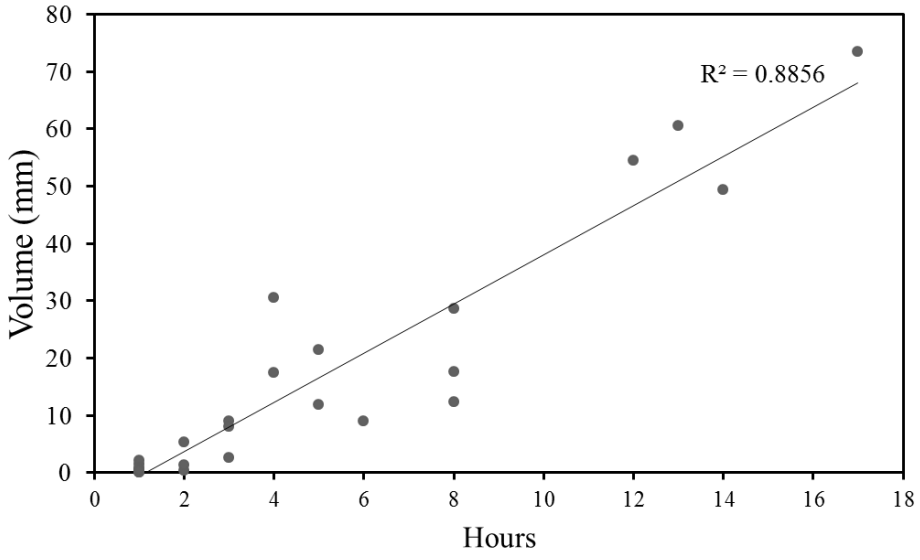

Figure 13: Rainstorm intensity for all 26 rainstorm events during 2014.

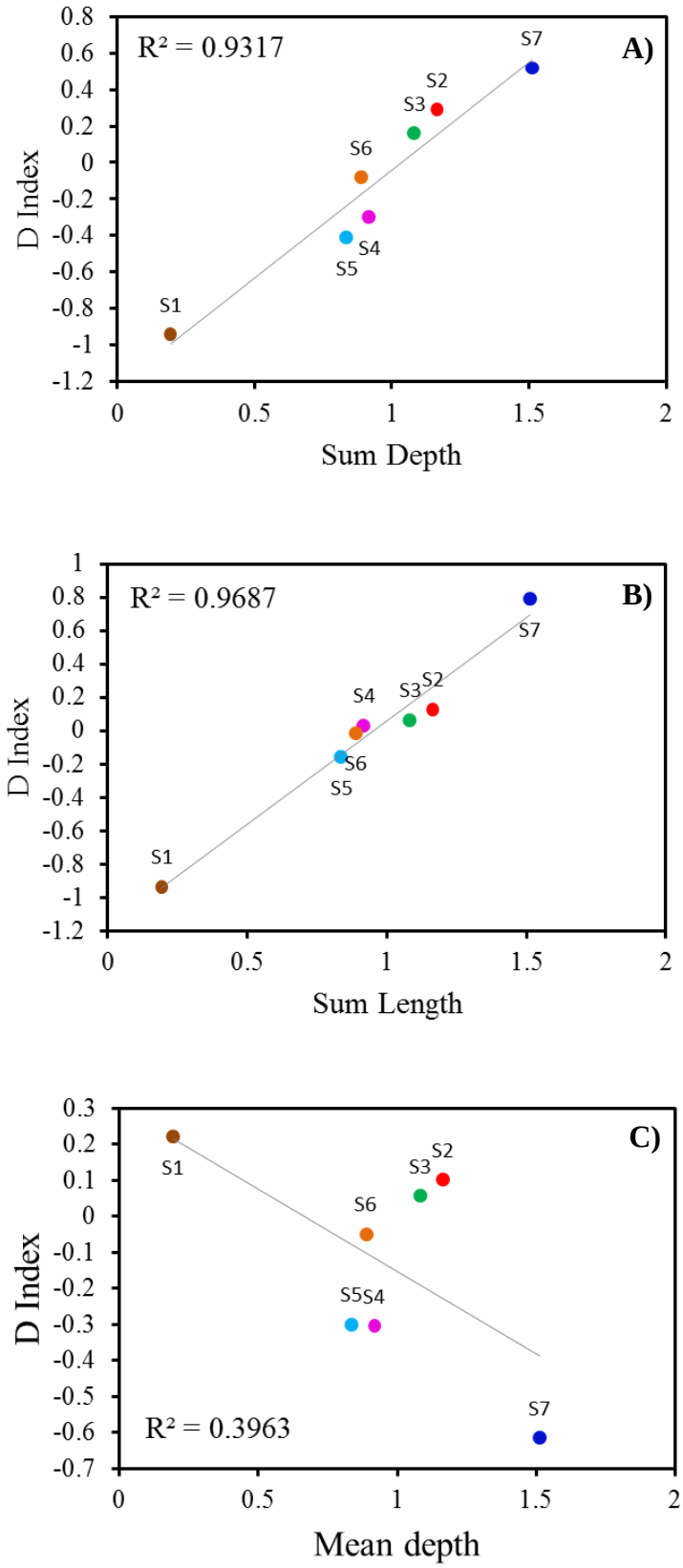

Figure 14: D Index as affected by each scenario. A) departure for sum depth; B) departure for sum length; and C) departure for mean depth.

A cross-section of a spatially random EG transect (from four transects tested) at the end of each scenario simulation is shown in Figure 15. The brown line represents S1. Since in this scenario almost no deepening occurred, it is analogous to the original DEM transect. Conversely, a considerable depth developed in the other scenarios. The lowest rainfall volume scenario (S5; -20%) deepened by 13.6 cm relative to the original DEM, while the scenarios with the highest rainfall volumes (S2 and S3), deepened by 45.5 cm. All scenarios exhibit foreseeable behavior as each increase in rainfall volume results in a deeper cross-section. However, the EG transect varies considerably between the different scenarios. This is especially true for the S6 and S7 cross-sections.

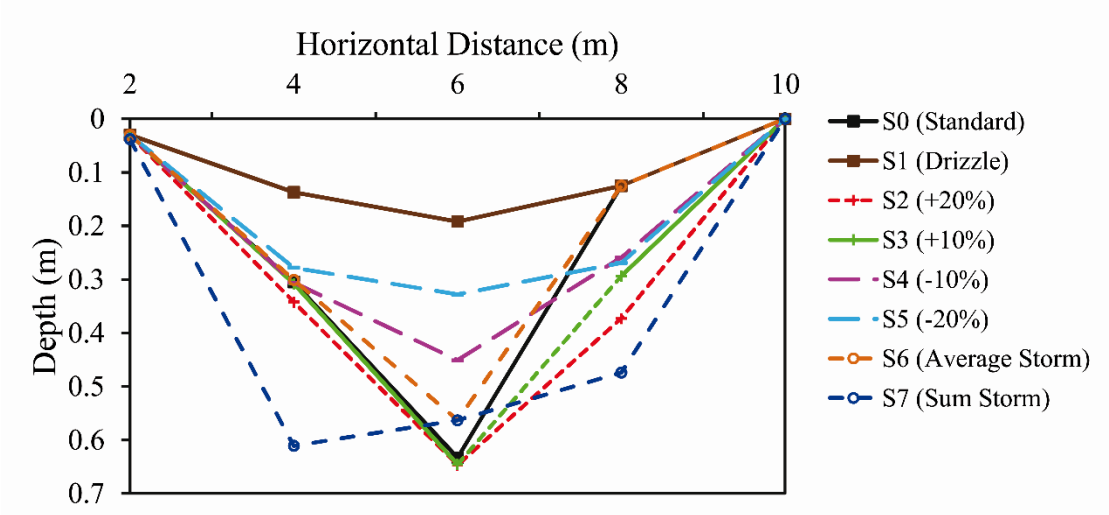

Figure 15: Cross-section for a randomly selected EG as affected by rainfall scenario changes. S1 (brown line) is analogous to the original DEM elevation, since no erosion occurred.

A part of the S6 cross-section overlaps with the original DEM, resulting in a narrower and slightly less deep gully compared to that resulting from the S0 simulation, while S7 resulted in a considerable wider transect which may be attributed to the lateral erosion process. The deepest point of the S7 cross-section deviates from the other deepest points of each scenario by horizontal distance of 2 meters. This could be attributed to variation in meandering (Coulthard and Van De Wiel, 2006). For the other scenarios (S2, S3, S4, S5) a dominant trend was observed - the deeper the transect, the wider it is. The two deepest cross-sections, yet with equal depth, are S2 and S3. This is somewhat unexpected given that S3 rainfall volume is 10% lower than S2. Another unexpected result is that S4 and S5 yield a wider gully than S0. Height-wise, the variances between the different cross-sections are reasonable (range of 50 cm).

The effect of each scenario on the four cross-sections was quantified using the Shoelace algorithm. It calculates the shape area of each transect as a constrained polygon e.g. if a cross-section is a V shaped than the algorithm calculates its area as an upside-down triangle. Table 5 shows the cross-section areas results for all scenarios for the four transects compared to the S0 shape area. Figure 16 shows the average change of each cross section according to each scenario. The results show that S1, S4 and S5 results in a smaller cross section than S0, while S2, S3 and S7 have generally larger cross section than S0.

Table 5: Summary of all four cross sections shape area response to each scenario compared to S0, using the shoelace algorithm.

	DEM	S0	S1	S2	S3	S4	S5	S6	S7
CS1	-0.54	0.00	-0.54	0.02	-0.04	-0.28	-0.35	0.08	0.10
CS2	-0.48	0.00	-0.48	0.06	0.04	-0.12	-0.40	-0.05	0.25
CS3	-0.45	0.00	-0.45	0.32	0.22	0.03	-0.10	-0.01	0.57
CS4	-0.39	0.00	-0.39	0.31	0.23	-0.14	-0.22	0.04	0.51

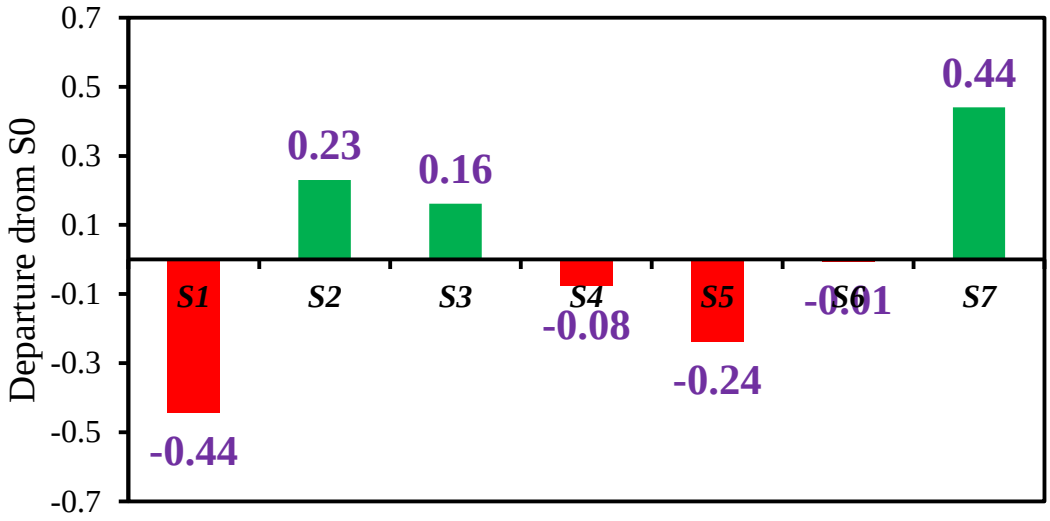

Figure 16: Differences of averaged cross-section area (Table 5) from S0 between each scenario, using the Shoelace algorithm. Solid red fill represent negative values and solid green fill, positive values.

Figure 17 presents the total cumulative sediment mass (Qs) transported via the basin's outlet, for each scenario for the entire season (normalized to the S0 Qs). Most scenarios present a similar trend, of two main inclination stages: first a substantial Qs increase in response to the first rainstorm which occurred in the 2nd week which contributes about 60% of the sediment flux. The second stage occurs during the 14th

week, contributing another 40%. However, S4 and S5 are only affected by the first rainstorm. As expected, S1 yielded a very low Qs: a 5% contribution form the 7th week. A strong correlation is found between rainfall volume change to sediment yield (r=0.98 for S2 to S5; Figure 12). Overall the results show that a 12 mm hour^{-1} rainfall intensity threshold is needed to initiate Qs generation. Further, at least two rainfall peaks within a singular storm are needed to produce sediment transport at the basin outlet (e.g. week 2 and 14). Conversely, storm events like week 4 and 5 which have a singular peak and a lower intensity than of 12 mm, did not yield any Qs.

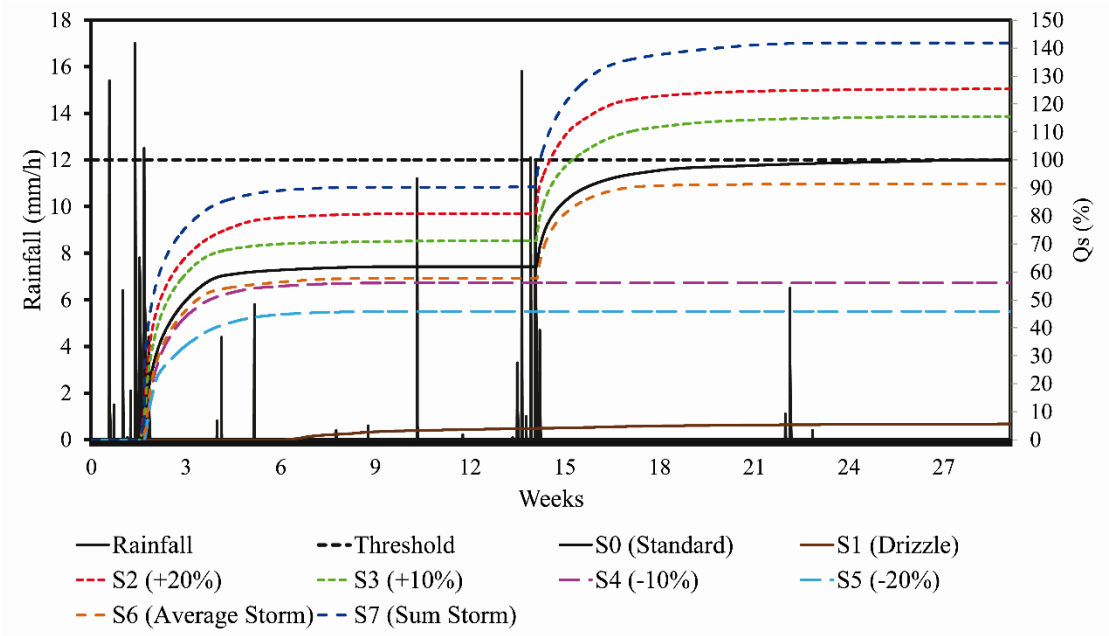

Figure 17: Accumulative sediment flux (Qs) during a rainfall season for each rainfall scenario. The black line represents the reference scenario (S0). Black bars represent rainfall distribution (for the S0 scenario) along the season. The dashed black line represents a threshold of 12mm rainfall which shows when exceeded, Qs is generated. It coincides with storms that at least have 2 peaks exceeding 12 mm.

3.3 Ephemeral Gullies Evolution Dynamics

The temporal change in mean depth (for eroded cells only; normalized against the S0 simulation) in weekly time steps is represented in Figure 18a. A substantial contribution of 60% in depth occurs during the 2nd week. By the 5th week the cumulative depth reached a value of 75% (red box). Another slight increase of roughly 15% can be noticed between the 15th and the 16th week. The actual depth values ranged from 0 to 14.9 cm. Figure 18b zooms in on the 2nd to 5th week period in hourly time steps. We plotted the rainfall behavior along the mean depth change. Towards the decay of each storm, mean depth value starts to increase. This lag is likely attributed to the nature of runoff generation mechanisms in semi-arid settings. As expected, there is a strong positive agreement between the volumes of the storm and the magnitude of mean depth change.

The evolutionary process of EG is presented using maps of elevation difference (ED) from the original DEM datum for the S0 simulation, at specific (dissimilar) time steps (Figure 19). The EG dynamics are shown to be divided into two stages. Stage 1: ranges from time step A to E, during which the longitudinal development of the gully network occurs. Almost 90% of the gully network length evolved during this stage in response to the rainstorm which occurred in the 2nd week. Stage 2: ranges from time step F to I, lasting for over a month, during which gully deepening occurs with minimal change to its aerial extent (i.e. change of depth value only). The change between time steps A to B best exemplifies the headcut migration process (Rengers and Tucker, 2014) occurring at the onset of the EG evolution process.

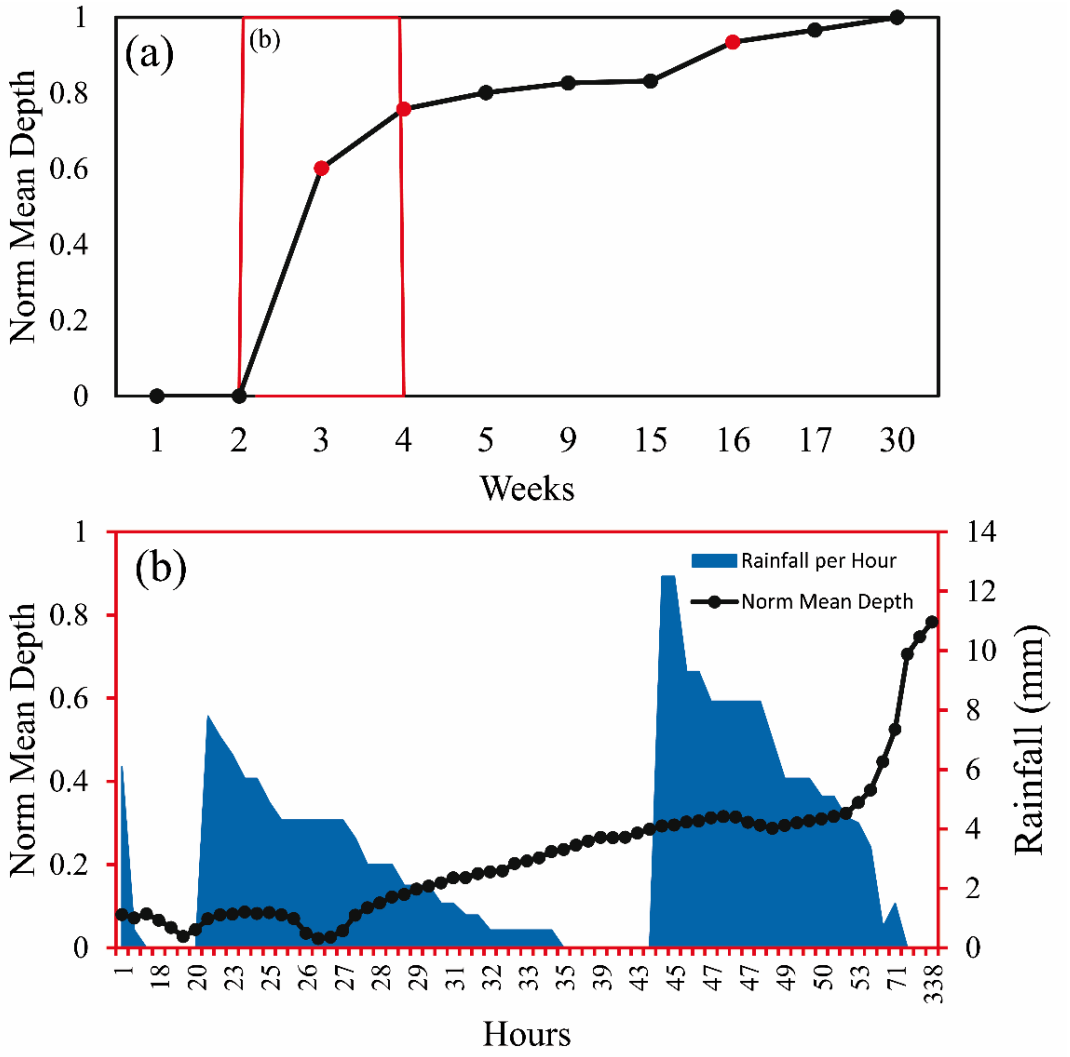

Figure 18: (a) Normalized mean depth change for each time step (scaled to weeks), according to the baseline scenario (S0). Red dots represent three considerable increases in mean depth. First, a 60% rise occurs in mean depth between week 2 and 3, and an additional 15% occurs between week 3 and 4. Following this, a 15% rise occurs between week 15 and 16. (b) The red box between week 2 and 4 in Figure 18a is expanded (rainfall was extracted respectively).

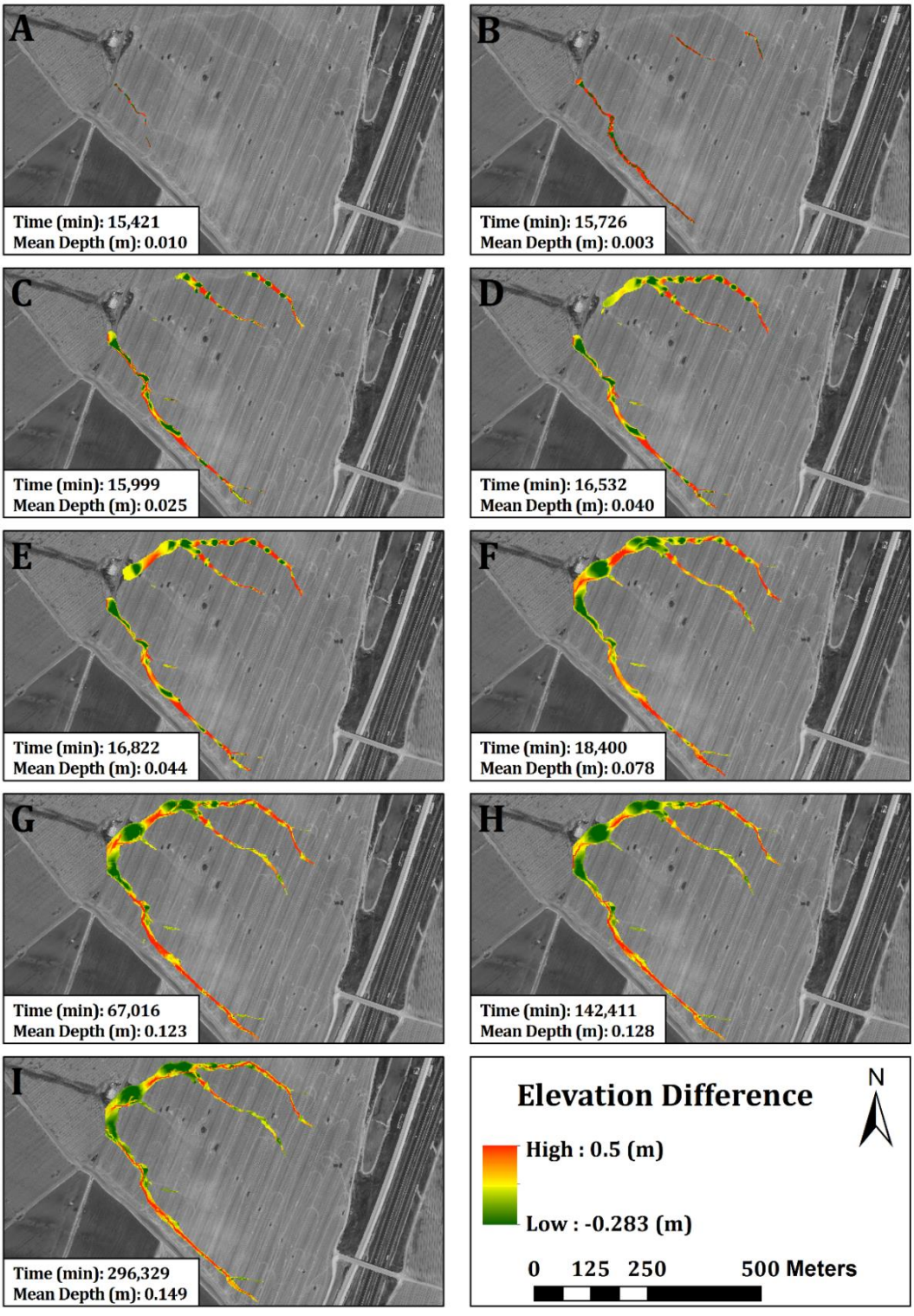

Figure 19: Temporal evolution during the S0 simulation for specific time steps along one rainfall season. Positive values represent erosion (red cells) while negative values represent deposition (green cells). The evolution is separated into two main stages: A to F – rapid aerial fluvial evolution with an average 1 to 4 cm deepening (along 12.5 days) and G to I – stable and expanding development with an average 10 cm deepening (along the rest of the season).

4. Discussion

In this paper we present a parameterization of short-scale ephemeral gully evolution simulations for the CL model. Calibration of CL is infrequent within the scientific literature. It is imperative to discuss the values of the parameterization procedure since they play a significant role in calibrating the model. A comparison between two previous studies and our results here regarding best suited values is presented in Table 2.

The ‘m’ parameter dictates whether modeled discharges are either flashy or moderate (Coulthard *et al.*, 2002). All three studies show that the 'm' value should be relatively high, around 0.01, as to represent long durational discharges, resulting in steadier simulations, as opposed to 0.005, which would cause flashier hydrographs. Although a lower m value is more intuitive to use with regard to ephemeral gullies, since these are typically triggered by extreme runoff events (Valentin *et al.*, 2005), it was found to substantially affect the erosion and deposition pattern, by yielding an excessive 'checkerboard’ pattern (Bates *et al.*, 2010). If we were to use a DEM with predefined drainage network (i.e. burned DEM discussed in section 2.3), a lower m value might be more adequate.

The discharge *Input/Output difference* which determines steady or non-steady operation, greatly affects the speed of simulations and here it is set at lower than the previous study (Hancock *et al.*, 2015). This is due to the short temporal scale simulated here resulting in a low mean annual flow value. Although CL was found to operate exceptionally faster using steady state flow, in some cases, it generated ‘checkerboard’ patterns as well. Using non-steady state flow simulations is more advisable, yet at a cost of exceedingly longer simulations (days as opposed to minutes) which may better represent the evolution process. The courant number is set

relatively low as well in this study. This originates from the necessity to maintain high stability in a short-scale spatial simulation. To summarize, the short temporal scale dictated the configuration of these parameters, as deviation from the suggested values lead to highly unstable simulations, resulting in unrealistic predictions.

The following parameters considerably differed between our parameterization and previously reported values, suggesting that these are more dominant in controlling short-term catchment dynamics: (i) Sediment transport formula; (ii) Lateral erosion rate; (iii) Maximum erode limit (MEL); (iv) Active layer thickness (ALT); and (v) Water depth threshold (WDT). We discuss these below.

The Wilcock and Crowe (2003) formula was found to be the only equation suitable for yielding satisfactory fluvial patterns. This may be due to the explicit particles size distribution used in this study as opposed to the aggregate size distribution measured via sieves in both previous studies (Coulthard *et al.*, 2012; Hancock *et al.*, 2015). This suggests that particle size-explicit formulations are important for EG simulations.

The lateral erosion parameter governs meandering and braided morphology patterns (Coulthard and Van De Wiel, 2006). We therefore chose to implement a relatively low value (0.0005) to enable more realistic micro-meandering and lesser deepening, as opposed to a value of 10 which would yield a narrower and deeper EG. As a result, width is overestimated in our simulations. This should be rethought as many studies describe EG as linear features or residing along permanent linear features (Valcarcel *et al.*, 2003).

MEL and ALT are intertwined parameters as both are components of the active layer system concept (Van De Wiel *et al.*, 2007). MEL determines the maximum elevation change allowed in each time step. ALT is suggested to be at least four times

higher than the MEL value (Van De Wiel *et al.*, 2007). We found that a fairly higher MEL value was needed to simulate a more rapid change with high sediment yield, which is more representative of ephemeral channels and short-temporal scale (Vanwalleghem *et al.*, 2005; Zhang *et al.*, 2014; Hancock *et al.*, 2014).

Although some reasoning was given for the fine tuning of each parameter, most of the parameters are derived from the DEM grid size, while the Manning roughness coefficient is not. To define the best suited Manning's *n* value for our study area, we adopted a ranking method proposed by Arcement Jr and Schneider (1989). Manning's n is composed of several elements which represent the actual roughness conditions that can be found in the field site. In this study, a Manning*'s n* value of 0.0396 was used. Similar values are found in other studies for fairly similar field conditions: 0.038 for irrigated surfaces and 0.034 for agricultural lands, after fall plowing without crops (Harun-ur-Rashid, 1990; Li and Zhang, 2001). Hancock et al. (2015) used a 0.04 n value as well, as it is suggested to be a default value. Given that our field site is an agricultural plot, i.e. highly erosive soils due to tillage, we used a relatively high *n* value.

Overall, rainfall patterns results were strongly correlated with changes in EG characteristics. For most rainfall scenarios, strong correlations were found to sum length, sum depth, mean depth and sediment flux (Figure 12, 14). Among all four, sediment flux and sum depth were found to be the most responsive to rainfall volume change. These findings are in agreement with previous studies (Nearing *et al.*, 2005; Chaplot, 2007; Arnaez *et al.*, 2007). However, the effect of lower rainfall volume scenarios (S4 and S5) on length and depth change were nearly double that of the high rainfall scenarios; 20% and 10% rainfall volume decrease yielded 41% and 30% decrease in depth, while 10% and 20% rainfall increase only yielded a 16% and 29%

depth increase (Table 4). This may be attributed to the fact that EG is a threshold driven phenomenon (Poesen *et al.*, 2003). EG dynamics will be minor below a certain rainfall threshold but will also not change dramatically with increasing rain volumes after that threshold is exceeded. Moreover, EG depth was found to be more sensitive to rainfall volume change relative to EG length. We propose that this is because length is controlled (constrained) by the basin topography (i.e. headwater slopes).

The S6 simulation (moderate rainfall intensity) resulted in changes of -1%, -8% and -4.9% in sum length, sum depth and mean depth respectively, relative to the S0 simulation (Figure 11). Further, analyzing sediment flux change (Figure 17) showed a similar trend of a -8.6% change compared to S0 simulation. This implies that a temporally average rainfall distribution (S6; Figure 7) does not greatly impact changes in EG characteristics for rainfall events with the same rainfall volume.

It can be deduced that sediment flux (Qs) behavior is affected by rainfall intensity, frequency and inter-storm rainfall distribution (Figure 17). This is to be inferred from Qs generation which occurs always where more than one peak storm event was reported. Nearing et al. (2005) showed that erosion (i.e. Qs in our case) is more likely to be influenced by rainfall in-storm intensity change than rainfall volume change alone. Figure 17 also showed that Qs flux at the basin outlet largely occurred during storms exceeding 12 mm hour^{-1}. Poesen et al. (2003) showed a relative similar threshold value regarding EGs (e.g. 14.5 mm to 22mm). Sediment flux in our simulations was found to be highly overestimated. This might be attributed to the *spin up* period within the model. Hancock et al. (2010) showed that during spin up, CAESAR typically exports small-fraction sediments from stream cells and smooth topographic features, resulting in a period of high magnitude sediment output which is not necessarily indicative of catchment dynamics. Although in their study, peak

sediment discharge was recorded after a few years, here it is analogous to a two week period after the season had started, compared with the rest of the year (Figure 17,18a). Further, in this study, soil description is immensely more detailed and composes mainly of much finer particles, as opposed to aggregates in the previous studies (Coulthard *et al.*, 2012; Hancock *et al.*, 2015).

The results in section 3.3 showed a partitioning of EG evolution into two stages; rapid EG network development and moderate deepening. This is, to some degree, in agreement with Gong et al. (2011), who concluded that EG erosion processes can be divided into two main periods: an initial adjustment followed by stable development. The transition between A to B in Figure 19 shows the headcut migration process (Rengers and Tucker, 2014). Headcut retreat is the process whereby the gully headcut migrates through propagation of dissecting upslope and excavating downslope the soil material from the surface prior to gullying above the gully head (Prasad and Romkens, 2003; Kirkby and Bracken, 2009). Figure 19 A, B and C also demonstrate that the EG is formed by a manner of discontinuous growth. This is in agreement with Bull's (1997) work that discusses the development of ephemeral streams in semiarid regions due to short term changes in environmental factors.

The promising results shown here are prone to input datasets limitations (with a strong emphasis on DEM). CL is strongly DEM dependent (Pasculli and Audisio, 2015). As a result, DEM artefacts can be a crucial problem using Cellular Automata models and thus can produce high uncertainty (Livne and Svoray, 2011). In some cases, artefacts are smoothed in CL simulations if slopes and discharge are low enough to allow both local erosion and deposition. However, if erosion predominates, DEM artifacts can generate channels that continue to evolve. DEM smoothing can reduce this problem but may not altogether remove it. On the other hand, as DEM

smoothing will result in a flatter terrain, it may skew the results towards a more depositional landscape. Another DEM control is its resolution. Here, CL overestimates width due to the relatively coarse spatial resolution of the DEM (2x2 m). EGs were found to expand to several cells, ranging from a single cell to about 10 at maximum (20 meters in length). If we take into account that the average width of all EGs in the plot site was measured as 2.2 m, then any gully that expanded to more than a single cell is automatically being overestimated. DEM can also affect the spatial predictive accuracy of the model. This problem is also propagated by biases in the field-survey (e.g. GPS accuracy). In some cases, CL predicted gullies matched those observed in aerial photos rather than those surveyed in the field. This is surprising since the DEM was surveyed in 2014 (corresponding to our simulations) while the aerial photo was taken in 2012. We conclude that GPS error lead to biases in our observational data. However, this discrepancy could also represent the ephemeral aspect of gullies, where EGs have evolved in a slightly different orientation yet adjacent to measured EGs. While in this study aerial digitized gullies were not used as a validation dataset, studies do incorporate digitized EGs as a measure of fit (Maugnard *et al.*, 2014). Further, during the field survey, the EGs were observed to be shallow and mostly covered in wheat crop remains, which reduced visibility and thus our ability to precisely identify where they end.

5. Conclusions

This paper demonstrates the viability of using a long-term oriented landform evolution model such as CAESAR-Lisflood (CL) to simulate an unstable transient phenomenon such as ephemeral gullies (EGs). CL yields a satisfactory predictive spatial fit to observed EGs while maintaining favorable realistic conditions such as network connectivity and narrow EGs. The simulations presented here demonstrate several known EG evolution mechanisms: discontinuous gullies, evolution periods and headcut migration. Achieving better correspondence is challenging yet promising as it is considerably controlled by the quality of the model's inputs.

The model was used to isolate and study the effects of rainfall characteristics on EG dynamics. The reference scenario (S0), once calibrated for one rainfall season, shows that EGs are mostly triggered by an initial period of intense fluvial processes driven by rainfall intensity threshold (12 mm $hour^{-1}$) and inner-storm reoccurrence. Both sediment flux and EG mean depth change reached 75% of the season-long flux shortly after the first two weeks. The rest of the scenarios which represented rainfall volume, duration and distribution change, show a high correlation between rainfall volume change to sediment yield and depth or length change. EG depth was found to be most responsive to rainfall characteristics compared to changes in EG length. This suggests that the EG network tends to reach near maximal extent at the start of the rainfall season under nearly any rainfall characteristics and that the effect of rainfall characteristics on EG-driven soil erosion is mostly due to deepening of these EGs. Lowering the rainfall volumes (compared to the baseline scenario) was found to affect EG length and depth by almost a factor of two greater than increasing the rainfall volumes. Inner storm analysis shows that moderate rainfall intensity induces

marginally less erosion compared to higher rainfall intensity, with the same rainfall volume.

The work presented here has significant and practical implications for improving our understanding of EG dynamics and its controlling factors. It demonstrates that the CL model is a robust modeling framework for investigating EGs and likely other short-term catchment processes. Future work will focus on investigating additional known EG controls such as vegetation, land use management and agricultural practices in various climatic setting and regions.

6. References

Agam A, Marder O, Barkai R. 2015. Small flake production and lithic recycling at Late Acheulian Revadim, Israel. *Quaternary International* **361**: 46-60. DOI: 10.1016/j.quaint.2014.06.070

Alonso C, Bennett S, Stein O. 2002. Predicting head cut erosion and migration in concentrated flows typical of upland areas. *Water Resources Research* **38**: 1303. DOI: 10.1029/2001WR001173

Arcement Jr G, Schneider V. 1989. Guide for Selecting Manning's Roughness Coefficients for Natural Channels and Flood Plains United States Geological Survey Water-supply Paper 2339. *pubs.usgs.gov/wsp/2339/report.pdf*

Arnaez J, Lasanta T, Ruiz-Flano P, Ortigosa L. 2007. Factors affecting runoff and erosion under simulated rainfall in Mediterranean vineyards. *Soil & Tillage Research* **93**: 324-334. DOI: 10.1016/j.still.2006.05.013

Bates PD, Horritt MS, Fewtrell TJ. 2010. A simple inertial formulation of the shallow water equations for efficient two-dimensional flood inundation modelling. *Journal of Hydrology* **387**: 33-45. DOI: 10.1016/j.jhydrol.2010.03.027

Beven K, Kirkby MJ. 1979. A physically based, variable contributing area model of basin hydrology. *Hydrological Sciences Journal* **24**: 43-69.

Boardman J, Poesen J. 2006. Soil erosion in Europe. Wiley Online Library: Chichester.

Bull W. 1997. Discontinuous ephemeral streams. *Geomorphology* **19**: 227-276. DOI: 10.1016/S0169-555X(97)00016-0

Capra A, Scicolone B. 2002. Ephemeral gully erosion in a wheat-cultivated area in Sicily (Italy). *Biosystems Engineering* **83**: 119-126. DOI: 10.1006/bioe.2002.0092

Chaplot V. 2007. Water and soil resources response to rising levels of atmospheric CO2 concentration and to changes in precipitation and air temperature. *Journal of Hydrology* **337**: 159-171. DOI: 10.1016/j.jhydrol.2007.01.026

Cohen S, Willgoose G, Hancock G. 2010. The mARM3D spatially distributed soil evolution model: Three-dimensional model framework and analysis of hillslope and landform responses. *Journal of Geophysical Research-Earth Surface* **115**: F04013. DOI: 10.1029/2009JF001536

Coulthard T, Van de Wiel M. 2013. Climate, tectonics or morphology: what signals can we see in drainage basin sediment yields?. *Earth Surface Dynamics* **1**: 13-27.

Coulthard TJ, Ramirez JA, Barton N, Rogerson M, Bruecher T. 2013a. Were Rivers Flowing across the Sahara During the Last Interglacial? Implications for Human Migration through Africa. *PloS one* **8**: e74834. DOI: 10.1371/journal.pone.0074834

Coulthard T, Van De Wiel M. 2006. A cellular model of river meandering. *Earth Surface Processes and Landforms* **31**: 123-132. DOI: 10.1002/esp.1315

Coulthard T, Lewin J, Macklin M. 2005. Modelling differential catchment response to environmental change. *Geomorphology* **69**: 222-241. DOI: 10.1016/j.geomorph.2005.01.008

Coulthard T, Macklin M, Kirkby MJ. 2002. A cellular model of Holocene upland river basin and alluvial fan evolution. *Earth Surface Processes and Landforms* **27**: 269-288. DOI: 10.1002/esp.318

Coulthard TJ, Hancock GR, Lowry JBC. 2012. Modelling soil erosion with a downscaled landscape evolution model. *Earth Surface Processes and Landforms* **37**: 1046-1055. DOI: 10.1002/esp.3226

Coulthard TJ, Neal JC, Bates PD, Ramirez J, de Almeida GAM, Hancock GR. 2013b. Integrating the LISFLOOD-FP 2D hydrodynamic model with the CAESAR model: implications for modelling landscape evolution. *Earth Surface Processes and Landforms* **38**: 1897-1906. DOI: 10.1002/esp.3478

De Santisteban L, Casali J, Lopez J. 2006. Assessing soil erosion rates in cultivated areas of Navarre (Spain). *Earth Surface Processes and Landforms* **31**: 487-506. DOI: 10.1002/esp.1281

de Vente J, Poesen J. 2005. Predicting soil erosion and sediment yield at the basin scale: Scale issues and semi-quantitative models. *Earth-Science Reviews* **71**: 95-125. DOI: 10.1016/j.earscirev.2005.02.002

de Vente J, Poesen J, Verstraeten G, Govers G, Vanmaercke M, Van Rompaey A, Arabkhedri M, Boix-Fayos C. 2013. Predicting soil erosion and sediment yield at regional scales: Where do we stand?. *Earth-Science Reviews* **127**: 16-29. DOI: 10.1016/j.earscirev.2013.08.014

Einstein HA. 1950. The bed-load function for sediment transportation in open channel flows. US Department of Agriculture

Evans R. 1993. On assessing accelerated erosion of arable land by water. *Soils and Fertilizers* **56**: 1285-1293.

Flores-Cervantes JH, Istanbulluoglu E, Bras RL. 2006. Development of gullies on the landscape: A model of headcut retreat resulting from plunge pool erosion. *Journal of Geophysical Research-Earth Surface* **111**: F01010. DOI: 10.1029/2004JF000226

Foster GR. 2005. Modeling ephemeral gully erosion for conservation planning. *International Journal of Sediment Research* **20**: 157-175.

Foster G. 1986. Understanding ephemeral gully erosion. *Soil Conservation: Assessing the National Resources Inventory.National Academy Press, Washington, DC*: 90-125.

Francipane A, Ivanov VY, Noto LV, Istanbulluoglu E, Arnone E, Bras RL. 2012. tRIBS-Erosion: A parsimonious physically-based model for studying catchment hydro-geomorphic response. *Catena* **92**: 216-231. DOI: 10.1016/j.catena.2011.10.005

Garcia-Ruiz JM, Begueria S, Nadal-Romero E, Gonzalez-Hidalgo JC, Lana-Renault N, Sanjuan Y. 2015. A meta-analysis of soil erosion rates across the world. *Geomorphology* **239**: 160-173. DOI: 10.1016/j.geomorph.2015.03.008

Gong JG, Jia YW, Zhou ZH, Wang Y, Wang WL, Peng H. 2011. An experimental study on dynamic processes of ephemeral gully erosion in loess landscapes. *Geomorphology* **125**: 203-213. DOI: 10.1016/j.geomorph.2010.09.016

Gordon LM, Bennett SJ, Bingner RL, Theurer FD, Alonso CV. 2007. Simulating ephemeral gully erosion in AnnAGNPS. *Transactions of the Asabe* **50**: 857-866.

Gvirtzman G, Wieder M, Marder O, Khalaily H, Rabinovich R, Ron H. 1999. Geological and pedological aspects of an Early-Paleolithic site: Revadim, Central Coastal Plain, Israel. *Geoarchaeology* **14**: 101-126.

Hancock GR, Lowry JBC, Coulthard TJ. 2015. Catchment reconstruction - erosional stability at millennial time scales using landscape evolution models. *Geomorphology* **231**: 15-27. DOI: 10.1016/j.geomorph.2014.10.034

Hancock GR, Willgoose GR, Lowry J. 2014. Transient landscapes: gully development and evolution using a landscape evolution model. *Stochastic Environmental Research and Risk Assessment* **28**: 83-98. DOI: 10.1007/s00477-013-0741-y

Hancock GR, Coulthard TJ, Martinez C, Kalma JD. 2011. An evaluation of landscape evolution models to simulate decadal and centennial scale soil erosion in grassland catchments. *Journal of Hydrology* **398**. DOI: 10.1016/j.jhydrol.2010.12.002

Hancock GR, Lowry JBC, Coulthard TJ, Evans KG, Moliere DR. 2010. A catchment scale evaluation of the SIBERIA and CAESAR landscape evolution models. *Earth Surface Processes and Landforms* **35**: 863-875. DOI: 10.1002/esp.1863

Harun-ur-Rashid M. 1990. Estimation of Manning's roughness coefficient for basin and border irrigation. *Agricultural Water Management* **18**: 29-33.

Huang CC, Pang J, Zha X, Su H, Zhou Y. 2012. Development of gully systems under the combined impact of monsoonal climatic shift and neo-tectonic uplift over the Chinese Loess Plateau. *Quaternary International* **263**: 46-54. DOI: 10.1016/j.quaint.2011.06.022

Ivanov V, Vivoni E, Bras R, Entekhabi D. 2004. Catchment hydrologic response with a fully distributed triangulated irregular network model. *Water Resources Research* **40**: W11102. DOI: 10.1029/2004WR003218

Kirkby MJ, Bracken LJ. 2009. Gully processes and gully dynamics. *Earth Surface Processes and Landforms* **34**: 1841-1851. DOI: 10.1002/esp.1866

Le Roux JJ, Sumner PD. 2012. Factors controlling gully development: Comparing continuous and discontinuous gullies. *Land Degradation & Development* **23**: 440-449. DOI: 10.1002/ldr.1083

Li Z, Zhang J. 2001. Calculation of field Manning's roughness coefficient. *Agricultural Water Management* **49**: 153-161. DOI: 10.1016/S0378-3774(00)00139-6

Livne E, Svoray T. 2011. Components of uncertainty in primary production model: the study of DEM, classification and location error. *International Journal of Geographical Information Science* **25**: 473-488. DOI: 10.1080/13658816.2010.517752

Maugnard A, Cordonnier H, Degre A, Demarcin P, Pineux N, Bielders CL. 2014. Uncertainty assessment of ephemeral gully identification, characteristics and topographic threshold when using aerial photographs in agricultural settings. *Earth Surface Processes and Landforms* **39**: 1319-1330. DOI: 10.1002/esp.3526

Merkel WH, Woodward DE, Clarke C. 1988. Ephemeral gully erosion model (EGEM)

Merritt W, Letcher R, Jakeman A. 2003. A review of erosion and sediment transport models. *Environmental Modelling & Software* **18**: 761-799. DOI: 10.1016/S1364-8152(03)00078-1

Munoz-Robles C, Reid N, Frazier P, Tighe M, Briggs SV, Wilson B. 2010. Factors related to gully erosion in woody encroachment in south-eastern Australia. *Catena* **83**: 148-157. DOI: 10.1016/j.catena.2010.08.002

Nachtergaele J, Poesen J, Steegen A, Takken I, Beuselinck L, Vandekerckhove L, Govers G. 2001. The value of a physically based model versus an empirical approach in the prediction of ephemeral gully erosion for loess-derived soils. *Geomorphology* **40**: 237-252. DOI: 10.1016/S0169-555X(01)00046-0

Nearing M, Jetten V, Baffaut C, Cerdan O, Couturier A, Hernandez M, Le Bissonnais Y, Nichols M, Nunes J, Renschler C, Souchere V, van Oost K. 2005. Modeling response of soil erosion and runoff to changes in precipitation and cover. *Catena* **61**: 131-154. DOI: 10.1016/j.catena.2005.03.007

Osem Y, Zangy E, Bney-Moshe E, Moshe Y, Karni N, Nisan Y. 2009. The potential of transforming simple structured pine plantations into mixed Mediterranean forests through natural regeneration along a rainfall gradient. *Forest Ecology and Management* **259**: 14-23. DOI: 10.1016/j.foreco.2009.09.034

Pasculli A, Audisio C. 2015. Cellular Automata Modelling of Fluvial Evolution: Real and Parametric Numerical Results Comparison Along River Pellice (NW Italy). *Environmental Modeling & Assessment*: 1-17.

Pimentel D, Harvey C, Resosudarmo P, Sinclair K, Kurz D, Mcnair M, Crist S, Shprotz L, Fitton L, Saffouri R, Blair R. 1995. Environmental and Economic Costs of

Soil Erasion and Conservation Benefits. *Science* **267**: 1117-1123. DOI: 10.1126/science.267.5201.1117

Poesen J, Vandekerckhove L, Nachtergaele J, Wijdenes DO, Verstraeten G, Van Wesemael B. 2002. 8 Gully Erosion in Dryland Environments. *Dryland Rivers: Hydrology and Geomorphology of Semi-arid Channels*: 229.

Poesen J. 2011. Challenges in gully erosion research. *Landform Analysis* **17**: 5-9.

Poesen J, Nachtergaele J, Verstraeten G, Valentin C. 2003. Gully erosion and environmental change: importance and research needs. *Catena* **50**: 91-133. DOI: 10.1016/S0341-8162(02)00143-1

Prasad S, Romkens M. 2003. Energy formulations of head cut dynamics. *Catena* **50**: 469-487. DOI: 10.1016/S0341-8162(02)00125-X

Rengers FK, Tucker GE. 2014. Analysis and modeling of gully headcut dynamics, North American high plains. *Journal of Geophysical Research-Earth Surface* **119**: 983-1003. DOI: 10.1002/2013JF002962

Soil Science Society of America. 2008. Glossary of Soil Science Terms 2008. ASA-CSSA-SSSA

Svoray T, Ben-Said S. 2010. Soil loss, water ponding and sediment deposition variations as a consequence of rainfall intensity and land use: a multi-criteria analysis. *Earth Surface Processes and Landforms* **35**: 202-216. DOI: 10.1002/esp.1901

Svoray T, Levi R, Zaidenberg R, Yaacoby B. 2015. The effect of cultivation method on erosion in agricultural catchments: integrating AHP in GIS environments. *Earth Surface Processes and Landforms* **40**: 711-725. DOI: 10.1002/esp.3661

Svoray T, Michailov E, Cohen A, Rokach L, Sturm A. 2012. Predicting gully initiation: comparing data mining techniques, analytical hierarchy processes and the topographic threshold. *Earth Surface Processes and Landforms* **37**: 607-619. DOI: 10.1002/esp.2273

Tucker GE, Hancock GR. 2010. Modelling landscape evolution. *Earth Surface Processes and Landforms* **35**: 28-50.

Valcarcel M, Taboada M, Paz A, Dafonte J. 2003. Ephemeral gully erosion in northwestern Spain. *Catena* **50**: 199-216. DOI: 10.1016/S0341-8162(02)00139-X

Valentin C, Poesen J, Li Y. 2005. Gully erosion: Impacts, factors and control. *Catena* **63**: 132-153. DOI: 10.1016/j.catena.2005.06.001

Van De Wiel MJ, Coulthard TJ, Macklin MG, Lewin J. 2007. Embedding reach-scale fluvial dynamics within the CAESAR cellular automaton landscape evolution model. *Geomorphology* **90**: 283-301. DOI: 10.1016/j.geomorph.2006.10.024

Vandaele K, Poesen J, Govers G, vanWesemael B. 1996. Geomorphic threshold conditions for ephemeral gully incision. *Geomorphology* **16**. DOI: 10.1016/0169-555X(95)00141-Q

Vanwalleghem T, Stockmann U, Minasny B, McBratney AB. 2013. A quantitative model for integrating landscape evolution and soil formation. *Journal of Geophysical Research-Earth Surface* **118**: 331-347. DOI: 10.1029/2011JF002296

Vanwalleghem T, Poesen J, Nachtergaele J, Verstraeten G. 2005. Characteristics, controlling factors and importance of deep gullies under cropland on loess-derived soils. *Geomorphology* **69**. DOI: 10.1016/j.geomorph.2004.12.003

Verachtert E, Van den Eeckhaut M, Poesen J, Deckers J. 2010. Factors controlling the spatial distribution of soil piping erosion on loess-derived soils: A case study from central Belgium. *Geomorphology* **118**: 339-348. DOI: 10.1016/j.geomorph.2010.02.001

Wilcock P, Crowe J. 2003. Surface-based transport model for mixed-size sediment. *Journal of Hydraulic Engineering-Asce* **129**: 120-128. DOI: 10.1061/(ASCE)0733-9429(2003)129:2(120)

Willgoose G, Bras R, Rodriguez-Iturbe I. 1991. A Coupled Channel Network Growth and Hillslope Evolution Model .2. Nondimensionalization and Applications. *Water Resources Research* **27**: 1685-1696. DOI: 10.1029/91WR00936

Woodward DE. 1999. Method to predict cropland ephemeral gully erosion. *Catena* **37**: 393-399. DOI: 10.1016/S0341-8162(99)00028-4

Zhang Q, Dong Y, Li F, Zhang A, Lei T. 2014. Quantifying detachment rate of eroding rill or ephemeral gully for WEPP with flume experiments. *Journal of Hydrology* **519**: 2012-2019. DOI: 10.1016/j.jhydrol.2014.09.040

Zhang Y, Wu Y, Lin B, Zheng Q, Yin J. 2007. Characteristics and factors controlling the development of ephemeral gullies in cultivated catchments of black soil region, Northeast China. *Soil & Tillage Research* **96**. DOI: 10.1016/j.still.2007.02.010

Ziliani L, Surian N, Coulthard TJ, Tarantola S. 2013. Reduced-complexity modeling of braided rivers: Assessing model performance by sensitivity analysis, calibration, and validation. *Journal of Geophysical Research-Earth Surface* **118**: 2243-2262. DOI: 10.1002/jgrf.20154

מבוא

זרימת נגר מרוכזת בשטחי ניקוז צרים גורמת לפחיתה משמעותית בעובי הקרקע ולהסעת סדימנטים במורד. הופעת ערוצונים זמניים, כסממן לאירועי סחיפת קרקע באגנים חקלאיים, היא תופעה נפוצה בעולם הידועה כבעלת השלכות הרסניות לקרקע וליבולים. במחקר זה נלמדו השפעות מאפייני הגשם (נפח, עוצמה וזמן) על התפתחות ערוצונים זמניים, בעזרת מודל התפתחות-נוף-פיזיקלי מפורש במרחב CAESAR-Lisflood. המודל חוזה את השתנות הנוף בהתאם למנגנוני סחיפה והשקעה באמצעות הדמיית מעבר תנועת מים במטריצת תאים. המודל כויל לשם לימוד וכימות מנגנון התפתחות ערוצונים זמניים בחלקה חקלאית קטנה (0.37 קמ״ר), באגן היקוות צחיח למחצה במרכז ישראל (רבדים), במשך עונת גשם אחת. המודל אומת כנגד עונת גשם נוספת ובהתאם למדידות מיקום וממדי ערוצונים תוך שימוש ב-GPS מדויק ותאודוליט אלקטרוני. הורצו שבעה תרחישי גשם: ארבעה תרחישים שונים בעובי הגשם בהתאם לעובי הגשם שנצפה לאותה שנה (20%-, 10%-,10%, 20%), ושלושה תרחישים שונים בהתפלגות העיתית של סופות הגשם על מנת לבודד את השפעת עוצמת הגשם על התפתחות הערוצונים. הממצאים מראים כי למודל יכולת חיזוי טובה במרחב בהשוואה להופעת הערוצונים בשטח. כמו כן, בחינה של עומקי הקרקע החזויים בממוצע, כנגד עומקי הקרקע המדודים, מראה התאמה טובה (כ-12.56 ס״מ כנגד 14.9 ס״מ בהתאמה). תוצאות מחקר זה מראות כי: 1) התפתחות הערוצונים הזמניים סווגה כמתרחשת בשני שלבים עיתיים דומיננטיים: א) התפתחות בקצב מהיר ולא יציב אשר מתרחשת למשך מספר ימים בודדים (כ- 75% ממשך ההתפתחות); ו-ב) העמקה מתונה למשך חודש, ולאחר מכן התייצבות ושימור למשך שארית העונה (25%); 2) התפתחות מיקרו-גאומורפולוגית משתנה בין התרחישים השונים, אשר תוצאתם בנפתולים שונים וברשת ניקוז (קישוריות) בעלת שונות גבוהה; 3) נמצאו מתאמים גבוהים בין עומק קרקע, אורך הערוצונים ושטף הסדימנטים בהם ובין שינוי בעובי הגשם ($r= 0.99, r=0.89 , r=0.98$) בהתאמה; 4) נצפתה הסעת סדימנטים במורד האגן כאשר נרשמת חריגה מעל ערך סף של 12 מ״מ גשם לשעה. למחקר משמעות יישומית שכן יש צורך רב בזיהוי אזורי סיכון לדלדול קרקע ולהבנה טובה יותר של התפתחות ערוצונים על מנת לתת מענה יעיל בשיטות שימור קרקע לתהליכי הסחיפה באגן.

מילות מפתח: סחיפת ערוצונים זמניים, CAESAR-Lisflood, דינמיקת זמן-מרחב, תרחישי גשם, אגנים חקלאיים.

תוכן עניינים

אוניברסיטת בן- גוריון בנגב

הפקולטה למדעי הרוח והחברה

המחלקה לגיאוגרפיה ופיתוח סביבתי

בחינת השפעת תרחישי גשם על דינמיקת זמן-מרחב קצרת טווח של התפתחות ערוצונים זמניים באגני היקוות חקלאיים בעזרת מודל התפתחות נוף

חיבור זה מהווה חלק מהדרישות לקבלת התואר "מוסמך למדעי הרוח והחברה" (M.A)

מאת: דודי הובר

מנחה: פרופסור טל סבוראי ודוקטור שגיא כהן

חתימת הסטודנט: _____ תאריך: 27.8.2015

חתימת המנחה: _____ תאריך: 27.8.2015

חתימת המנחה: _____ תאריך: 27.8.2015

חתימת יו"ר הועדה המחלקתית: _____ תאריך: _____

ספטמבר, 2015

אוניברסיטת בן- גוריון בנגב

הפקולטה למדעי הרוח והחברה

המחלקה לגיאוגרפיה ופיתוח סביבתי

בחינת השפעת תרחישי גשם על דינמיקת זמן-מרחב קצרת טווח של התפתחות ערוצונים זמניים באגני היקוות חקלאיים בעזרת מודל התפתחות נוף

חיבור זה מהווה חלק מהדרישות לקבלת התואר "מוסמך למדעי הרוח והחברה" (M.A)

מאת: דודי הובר

בהנחיית: פרופסור טל סבוראי ודוקטור שגיא כהן

תשרי תשע"ה ספטמבר 2015